# Prenatal vitamin D deficiency alters immune cell proportions of young adult offspring through alteration of long-term stem cell fates

*Koki Ueda[1,2], *Shu Shien Chin[3], *Noriko Sato[4], Miyu Nishikawa[5], Kaori Yasuda[6], Naoyuki Miyasaka[7], Betelehem Solomon Bera[8], Laurent Chorro[3], Reanna Doña-Termine[8], Wade R Koba[9], David Reynolds[8], Ulrich G. Steidl[1,10,11,13], Gregoire Lauvau[3], John M. Greally[8,12], Masako Suzuki[8,14$]

1. Department of Cell Biology, Albert Einstein College of Medicine, 1300 Morris Park Ave, Bronx, NY, 10461, USA
2. Department of Blood Transfusion and Transplantation Immunology, Fukushima Medical University, 1 Hikarigaoka, Fukushima, Fukushima, 960-1295, Japan
3. Department of Microbiology & Immunology, Albert Einstein College of Medicine, 1301 Morris Park Ave, Bronx, NY, 10461, USA
4. Department of Food and Nutrition, Faculty of Human Sciences and Design, Japan Women's University, 2-8-1 Mejirodai, Bunkyo-ku, Tokyo 112-8681, Japan
5. Department of Biotechnology, Faculty of Engineering, Toyama Prefectural University, 5180 Kurokawa, Imizu, Toyama, 939-0398, Japan
6. Department of Pharmaceutical Engineering, Faculty of Engineering, Toyama Prefectural University, 5180 Kurokawa, Imizu, Toyama, 939-0398, Japan
7. Graduate School of Medical and Dental Sciences, Medical and Dental Sciences, Systemic Organ Regulation, Comprehensive Reproductive Medicine, Tokyo Medical and Dental University, Bunkyo-ku, Tokyo
8. Department of Genetics, Albert Einstein College of Medicine, 1301 Morris Park Ave, Bronx, NY, 10461, USA
9. Department of Radiology, Albert Einstein College of Medicine, 1300 Morris Park Ave, Bronx, NY, 10461, USA

26 10. Ruth L. and David S. Gottesman Institute for Stem Cell Research and Regenerative Medicine,
27 Albert Einstein College of Medicine, 1300 Morris Park Ave, Bronx, NY 10461, USA
28 11. Department of Oncology, Albert Einstein College of Medicine – Montefiore Medical Center, 1300
29 Morris Park Ave, Bronx, NY 10461, USA
30 12. Department of Pediatrics, Albert Einstein College of Medicine – Montefiore Medical Center, 1300
31 Morris Park Ave, Bronx, NY 10461, USA
32 13. Montefiore-Einstein Cancer Center, Albert Einstein College of Medicine – Montefiore Medical
33 Center, 1300 Morris Park Ave, Bronx, NY 10461, USA
34 14. Department of Nutrition, Texas A&M University, 2253 TAMU, College Station, TX, 77840, USA
35 * Equal contribution
36 $Corresponding author
37 Masako Suzuki
38 Tel:+1-979-847-8714
39 E-mail: masako.suzuki@ag.tamu.edu

**ABSTRACT**

Vitamin D deficiency is a common deficiency worldwide, particularly among women of reproductive age. During pregnancy, it increases the risk of immune-related diseases in offspring later in life. However, exactly how the body remembers exposure to an adverse environment during development is poorly understood. Herein, we explore the effects of prenatal vitamin D deficiency on immune cell proportions in offspring using vitamin D deficient mice established by dietary manipulation. We found that prenatal vitamin D deficiency alters immune cell proportions in offspring by changing the transcriptional properties of genes downstream of vitamin D receptor signaling in hematopoietic stem and progenitor cells of both the fetus and adults. Our results suggest the role of cellular differentiation properties of the hematopoiesis as the long-term memories of prenatal exposure at the adult stage. Moreover, further investigations of the associations between maternal vitamin D levels and cord blood immune cell profiles from 75 healthy pregnant women and their term babies also confirm that maternal vitamin D levels in the second trimester significantly affect immune cell proportions in the babies. This highlights the importance of providing vitamin D supplementation at specific stages of pregnancy.

## INTRODUCTION

Vitamin D, a micronutrient/hormone, regulates transcription by binding to its nuclear receptor, the vitamin D receptor (VDR). Humans can obtain vitamin D through photosynthesis on the skin and food intake. Approximately 50% to 90% of vitamin D is synthesized on the skin via sunlight exposure, while the remainder comes from the diet. Cutaneous vitamin D synthesis depends on environmental factors (geographic latitude, season, and amount of air pollution), skin type, clothing habitats, and lifestyle[1]. Despite country-level vitamin D fortification programs in many countries, the prevalence rate of vitamin D deficiency, especially in reproductive-age women[2–7], is still high worldwide[8–14]. The most severe consequence of vitamin D deficiency is rickets or impaired bone formation (reviewed by Holick[15]). Besides its importance in bone formation, VDR signaling regulates gene transcription in nearly every tissue in our bodies, including the brain, heart, muscle, kidney, and immune system (reviewed in Pike et.al[16]). During development, the micronutrient status of offspring is entirely dependent on the status of the mother; therefore, developing embryos are vulnerable to adverse micronutrient conditions of deficient mothers[17–21]. To study the adverse consequences of prenatal vitamin D exposure, animal models with maternal dietary manipulations[22–35] and knockout mouse model studies[18,36–42] have been utilized. Studies using knockout mice models have shown that depletion of VDR causes a rickets-like phenotype after weaning. Both maternal dietary manipulation and knockout mouse models revealed that prenatal vitamin D deficiency can lead to immune defects in offspring. Epidemiological studies in humans have demonstrated that prenatal vitamin D deficiency has been associated with susceptibility to a number of immune-related diseases affecting their children, including asthma[43,44], multiple sclerosis[45], and type I diabetes[46–48]. These findings indicate that prenatal vitamin D deficiency disturbs immune cell development. In addition, it is possible that the hematopoietic system poses a long-term memory of exposure to vitamin D deficiency during development. However, this memory mechanism has not been extensively studied.

80 In this work, we show that prenatal vitamin D deficiency alters immune cell proportions of offspring
81 during adulthood, attributed to cell fate decisions influenced by transcriptional alterations of VDR
82 signaling pathway genes. Our data also supports that changing the cell fate of stem cells is the key
83 component of the long-term effects of maternal vitamin D deficiency on the hematopoietic system of
84 offspring.
85
86 **RESULTS:**
87 Lack of impact of maternal vitamin D deficient diet feeding on offspring bone development
88 We summarized the dietary intervention strategy in **Fig. 1**. We randomly assigned six weeks old female
89 C57BL/6J mice to a vitamin D-sufficient diet (VDsuf,1.0 IU/g vitamin D) and a vitamin D-deficient diet
90 (VDdef, 0.0 IU/g vitamin D) for five weeks prior to mating with control diet-fed C57BL/6J male mice. The
91 daily food intakes of each diet were comparable between the VDsuf and VDdef. To prevent hypocalcemia,
92 the VDdef group received 1.5% calcium gluconate in their drinking water during the VDdef diet feeding.
93 After five weeks of feeding VDdef, serum vitamin D (25-hydroxyvitamin $D_3$, 25(OH)$D_3$) concentrations of
94 the VDdef-fed females reached the vitamin D deficient threshold (5.1±3.8 ng/mL, n=8), which is about
95 6.5 times lower than that of the VDsuf-fed females (33.0±5.44 ng/mL, n=10) (**Supplementary Fig. 1A**).
96 After delivery, all female mice were fed VDsuf. While the number of offspring per dam was smaller in
97 VDdef-fed females (mean = 3.82, standard deviation (sd) = 2.8, n=16) than in VDsuf-fed females
98 (mean=4.7, sd=1.7, n=10), the difference was not significant (p=0.32). We did not observe any obvious
99 adverse effects of VDdef diet feeding on these female mice prior to or during their pregnancy. All offspring
100 were fed VDsuf after weaning and maintained the diet until the sampling. The growth of VDdef-fed female
101 offspring (VDD) and VDsuf-fed female offspring (VDS) based on their body weight were comparable for
102 all of the time points we measured: postnatal day 1 (PD1) (n=9 VDS and n=11 VDD), 5, 9, and 13 weeks
103 of age (n=40 VDD and n=27 VDS) (**Supplementary Fig. 1B and 1C**). While VDD males were slightly
104 smaller than VDS males, as Seipelt et al. reported[49], the difference was not statistically significant at all
105 time points. This discrepancy could be attributed to the differences in diet used or calcium

106 supplementation to VDdef-fed mothers. The serum vitamin D concentrations of VDD were lower than the
107 detection limit (0.6 ng/ml, n=3 per group) at PD1 (**Supplementary Fig. 1A**). While the serum vitamin D
108 concentration of VDD was still significantly lower than that of VDS (n=5 per group) at five weeks of age,
109 their status was not deficient anymore (**Supplementary Fig. 1A**). We collected tissues and weighted
110 liver, lung, kidney, thymus, spleen, and heart from the VDD and VDS at 16 weeks of age (16 wks) (n=4-
111 6 for each group). The average body weight adjusted tissue weights were not significantly different
112 between the groups, except the heart was heavier in male VDD compared to male VDS (p=0.041)
113 (**Supplementary Fig. 1D**). We also assessed the bone and tissue mineral density of the humerus of the
114 left arm of the offspring using an X-ray CT system at 16 wks (n=5-6 males for each group). Bone volume,
115 bone mineral content, bone mineral density, tissue mineral content, tissue mineral density, and bone
116 volume fraction were assessed, and no significant alterations were observed (**Supplementary Fig. 1E**).
117

118 <u>Prenatal vitamin D deficiency decreases CD4+ and CD8+ T cell proportions of the offspring in peripheral</u>
119 <u>blood and spleen</u>

120 We collected peripheral blood from VDD and VDS and compared the immune cell profiles at 16 wks
121 (n=11 per group). We observed a significant reduction of CD4+ T cells (28.2% decrease at p=0.0018)
122 and CD8+ T cells (14.7% decrease at p=0.037) in VDD males compared to VDS males (**Fig. 2a**). This
123 reduction was not observed in females (**Supplementary Fig. 2**). We also compared the immune cell
124 profiles of spleen (n=6 per group) and observed the significant reduction of CD4+ T cells (18.4% decrease
125 at p=0.0035) and CD8+ T (11.1% decrease at p=0.026) cells in VDD (**Fig. 2b**). Representative flow
126 cytometry traces are shown in **Supplementary Fig. 3.**
127

128 <u>The reduced proportion of lymphocytes in the periphery reflects the cellular composition changes in the</u>
129 <u>bone marrow.</u>

130 During hematopoiesis, hematopoietic stem cells (HSCs) undergo differentiation into three multipotent
131 progenitor cells (MPP2, MPP3, and MPP4) in the bone marrow in adults[50]. MPP2 and MPP3 are further

132 differentiated primarily into the myeloid lineage, while MPP4 is into the lymphoid lineage. MPP2 is biased
133 toward producing megakaryocytes and erythrocytes, and MPP3 towards granulocytes and
134 macrophages[50]. To test if the T cell reductions in the periphery are reflected in the alterations in bone
135 marrow, we collected mononucleated cells from bone marrow from the offspring at 16wks (n=9-10 per
136 group). The total number of bone marrow mononucleated cells in VDD was significantly decreased
137 compared to VDS (3,354,105±439,109 and 2,215,799±353,525 in VDS (n=10) and VDD (n=10),
138 respectively, p=0.000013, **Fig. 3a**). We, then analyzed the proportions of HSCs, MPPs, and
139 hematopoietic progenitor cells using the previously reported definitions[50,51]; lineage negative (Lin-, CD3-
140 /CD4-/CD8-/B220-/Ter119-/CD11b-/Gr-1-/CD127-), Lin-/Sca-1+/c-Kit+ (LSK), long-term hematopoietic
141 stem cell (LT-HSC, LSK/Flk2-/CD150+/CD48-), short-term hematopoietic stem cell (ST-HSC, LSK/Flk2-
142 /CD150-/CD48-), multipotent progenitor 2 (MPP2, LSK/Flk2-/CD150+/CD48+), multipotent progenitor 3
143 (MPP3, LSK/Flk2-/CD150-/CD48+), multipotent progenitor 4 (MPP4, LSK/Flk2+), common myeloid
144 progenitor cells (CMP, Lin-/c-Kit+/CD34+/CD16/32-), common lymphoid progenitor cells (CLP, Lin-/c-
145 Kit+/Flk2+/CD127+), granulocyte-monocyte progenitor cells (GMP, Lin-/c-Kit+/CD34+/CD16/32+),
146 megakaryocyte-erythrocyte progenitor cells (MEP, Lin-/c-Kit+/CD34-/CD16/32-), and Lin-/CD127+ (early
147 T cell progenitor). We observed a significant reduction (48.9% decrease) in the absolute number of LSK
148 (565,312±153,178 and 289,052±91,984 in VDS and VDD, respectively, p=0.00023, **Fig. 3b**). While the
149 p-value (p=0.078) didn't pass our significant threshold, the proportion (%) of LSK in the live bone marrow
150 mononucleated cells was also decreased in VDD mice (0.19±0.04% and 0.16±0.05% in VDS (n=10) and
151 VDD (n=9), respectively, **Supplementary Fig. 4a**). As the absolute number of LSK decreased in VDD,
152 the absolute numbers of HSCs, MPPs, and progenitors were also decreased (**Fig. 3c and d**). Among the
153 MPPs, MPP4 was the only MPP that significantly reduced in both absolute numbers (413,267± 127,529
154 and 190,922± 49,401 in VDS (n=10) and VDD (n=9), respectively, p=0.0027, **Fig. 3c**) and the proportion
155 of the live bone marrow mononucleated cells (0.14±0.03% and 0.10±0.02% in VDS and VDD,
156 respectively, p=0.0096, **Supplementary Fig. 4b**). Among the progenitor cells, the absolute numbers of

157 CMP, GMP, CLP, and Lin-/CD127+ were significantly reduced in VDD (n=9) compared to VDS (n=9) (**Fig.**
158 **3d**). Interestingly, while the proportional averages of Lin-/CD127+ (p=0.07) and CLP (p=0.19) were
159 decreased, the proportion of GMPs was increased in VDD compared to VDS (50.1% increase, p=0.001,
160 **Supplementary Fig. 4c**). Representative flow cytometry traces are shown in **Supplementary Fig. 5.**
161

162 Prenatal vitamin D deficiency alters gene expression profiles of MPP4 cells

163 We performed transcriptome analysis on bone marrow MPP4 from VDD and VDS to see the
164 transcriptional alterations at 16 weeks of age (n=3 per group). The sequencing status and quality of each
165 sample are summarized in **Supplementary Data 1**. All samples have passed primary quality checks. A
166 hierarchical clustering analysis showed a clear dissociation, suggesting genome-wide transcriptional
167 alterations in VDD (**Fig. 4a**). We identified 612 differentially expressed genes (DEGs) with at least 1.2-
168 fold change and a false discovery rate adjusted p-value (FDR-adj p-value) <0.05 (**Fig. 4b,**
169 **Supplementary Data 2**). Of those, 345 were upregulated, and 267 were downregulated. The Gene
170 Ontology (GO) enrichment analysis of upregulated genes revealed enrichment of genes related to
171 leukocyte migration and chemotaxis (**Fig. 4c left**), while downregulated genes showed enrichment in the
172 homeostasis of cell numbers and regulation of hemopoiesis (**Fig. 4d left, Supplementary Data 3**). The
173 Gene-Concept Network analysis revealed that hematopoietic transcription factors, including *Lmo2*, *Tal1*,
174 *Gata2*, and *Mpl*, were downregulated and were found to overlap in the top five enriched GO terms (**Fig.**
175 **4d right**). Transcription factor (TF) Perturbations Followed by Expression analysis
176 (https://maayanlab.cloud/Enrichr/) revealed that the detected DEGs were enriched in the genes perturbed
177 in LSK of the hematopoietic transcription factor knockout models in the same directions. The upregulated
178 genes were enriched in NFIX (GSE45492) [52] and SRF (GSE23556) [53] knockouts upregulated genes
179 (adjusted p-value=3.92E-47 and 9.15E-29, respectively) and downregulated genes were enriched in
180 NFIX and SRF knockout downregulated genes (adjusted p-value=1.98E-36 and 4.55E-12, respectively)
181 (**Supplementary Fig. 6**). Gene Set Enrichment Analysis (GSEA) showed leukocyte differentiation
182 (GO:0002521, enrichment score = 0.385, q-value= 0.010), lymphocyte differentiation (GO:0030098,

183 enrichment score = 0.412, q-value= 0.026), T cell differentiation (GO:0030217, enrichment score =0.435,
184 q-value=0.023) were enriched (**Supplementary Data 4**). This result suggests that prenatal vitamin D
185 deficiency induces long-term transcriptional alterations in hematopoietic stem cells that persist into
186 adulthood.
187
188 Prenatal vitamin D deficiency alters cellular compositions of the embryonic day 14.5 (e14.5) embryonic
189 liver, suggesting immune cell proportion changes start during development.
190 To assess if the cell composition alteration started at the embryonic stage, we performed single-cell RNA-
191 seq (scRNA-seq) on the e14.5 fetal liver of both VDS and VDD embryos using the 10x Genomics
192 Chromium platform (n=3 per group). Multiplexing with cell hash antibodies was used to reduce the
193 technical batch effect. The obtained sequences were aligned by the 10x Genomics software, CellRanger,
194 and the matrix was demultiplexed and analyzed by Seurat, an R-package [54–56]. After eliminating low-
195 quality cells (<1000 genes/cell, <5000 reads/cell, and >10% mitochondrial reads/cell) and cells without
196 cell hashing information, we have identified 21 different cell clusters in a total of 6947 cells. We identified
197 the cell types of each cell cluster based on the marker gene expression status (**Fig. 5a, Supplementary**
198 **Data 5**). We detected three HSC/MPP populations, lineage-specific progenitor cells, erythroid lineage
199 cells, and hepatoblast cells in e14.5 liver. Concordant with the previous report[57], more than half of the
200 cells were identified as erythroid lineage cells. The cellular composition analysis showed that one of the
201 HSC/MPP populations (HSC/MPP 1) was significantly increased in VDD embryos, and two erythroid
202 lineage cells (Early Erythroid 1 and Erythroid 3) were decreased (**Fig. 5b**), suggesting the cell
203 composition changes started at least at the embryonic stage. A pseudo bulk RNA-seq analysis on the
204 scRNAseq datasets showed that down-regulated genes were enriched in the genes regulated by
205 hematopoietic system transcription factors (**Fig. 5c, Supplementary Data 6-8**). Among these
206 transcription factors, *Tal1*, *Lmo2, Meis1*, and *Erg* were also identified as VDD downregulated genes in
207 MPP4 at the adult stage (**Supplementary Data 2**). To test whether vitamin D alters the expression of
208 these genes, we measured the expression of *Tal1*, *Lmo2,* and *Erg*, the known hematopoietic transcription

209 factors, by quantitative RT-PCR on an embryonic stem cell-derived hematopoietic progenitor cell line,
210 HPC-7[58], after treating 1-alpha-25-dihydroxyvitamin $D_3$, a ligand of VDR, or ethanol (solvent) for 24 hours
211 by quantitative RT-PCR (**Fig. 4d**). We observed a significant increase of *Lmo2* (p=0.034) and *Erg*
212 (p=0.005) expression. This result suggests that the gene expression alterations observed at e14.5 were
213 attributed to the dysregulation of hematopoietic transcription factors, such as *Lmo2* and *Erg,* regulated
214 by VDR signaling pathways.
215
216 <u>Maternal serum vitamin D status in the second trimester is positively associated with the CD8+ T cell</u>
217 <u>proportion in the cord blood.</u>
218 To test the associations between maternal vitamin D levels and immune cell proportions of offspring, we
219 assessed 75 pregnant Japanese women who were recruited as participants of The Birth Cohort Gene
220 and Environment Interaction Study of TMDU (BC-GENIST) project at the Tokyo Medical and Dental
221 University, Bunkyo, Tokyo, Japan[59,60]. The study was approved by the Institutional Review Board of
222 Tokyo Medical and Dental University (No. G2000-181, 29 July 2014). We measured the concentration of
223 serum 25(OH)$D_3$ at two-time points: time point 1 (T1), intended to represent the second trimester from
224 week 10 to week 29, and time point 2 (T2), to represent the third trimester from week 33 to week 40 of
225 gestational age. The immune cell proportions were estimated from the bulk DNA methylation profiles of
226 the cord blood of the fetus using a Bioconductor package FlowSorted.CordBloodCombined.450k[61–64].
227 We excluded one participant who did not have T1 serum 25(OH)$D_3$ status from the analysis. The
228 demographic, clinical, and phenotypic information for the study participants is provided in **Table 1**. All
229 participants are healthy pregnant Japanese women without smoking or drinking during their pregnancy.
230 No participants had hypertension. The average maternal age at delivery was 34.2 (sd 4.0) years old, with
231 pre-pregnancy BMI 17.1-29.2 (average 20.73, sd 2.6). 70.3% of women took prenatal vitamin
232 supplements, and the average estimated daily dietary vitamin D intake was 5.1 (sd 4.4) μg/day[65,66]. 34
233 offspring were males (45.9%), and the average gestational week of the delivery was 39.1 (sd 1.2). The

234 average concentration of serum 25(OH)$D_3$ was 25.2 (sd 11.8) ng/ml in the second trimester (average
235 gestation week 19.0 (sd 4.5), T1) and 28.0 ng/ml (sd 14.4) in the third trimester (average gestation week
236 35.9 (sd 0.9), T2). 30 participants were vitamin D deficient (serum 25(OH)$D_3$ <20 ng/ml) at T1 (40.5%),
237 and 23 were vitamin D deficient at T2 (31.8%). Of those, eight participants were vitamin D deficient at
238 both T1 and T2. While we observed significant associations between the serum 25(OH)$D_3$ levels and
239 sampling season (Summer and Winter) ($p=0.047$ and $p<0.001$, T1 and T2, respectively), no significant
240 associations were observed in maternal age, pre-pregnancy BMI, sex of fetuses, prenatal vitamin
241 supplements usage and dietary vitamin D intake. The results of the univariate model fitting are shown in
242 **Supplementary Data 9**. To analyze the associations between maternal serum 25(OH)$D_3$ levels and
243 immune cell profiles of the cord blood, we calculated principal components (PCs) of immune cell profiles
244 and assessed the contributions of each covariate. Gestation weeks at delivery showed the most
245 significant contributions to PC1 ($p= 0.0063$ and adjusted $r^2=0.087$) and PC2 ($p= 0.000027$ and adjusted
246 $r^2=0.208$), followed by maternal serum 25(OH)$D_3$ at T1 to PC1 ($p= 0.021$ and adjusted $r^2=0.059$) and
247 being born in summer ($p= 0.049$ and adjusted $r^2=0.04$) (**Fig. 6a**). We then assessed the associations of
248 covariates to each cell type. We observed that the gestational weeks at delivery were negatively
249 associated with the proportions of CD4 T cells (estimate -0.027 and $p=0.00006$) and B cells (estimate -
250 1.12 and $p=0.00002$) and positively associated with proportions of granulocytes (estimate 0.028 and
251 $p=0.0014$). Maternal serum 25(OH)$D_3$ at T1 was positively associated with proportions of CD8 T cells
252 (estimate 0.0007 and $p=0.0216$) and monocytes (estimate 0.0005 and $p=0.0349$) and negatively
253 associated with proportions of granulocytes (estimate -0.0024 and $p=0.0365$) (**Supplementary Fig. 7**).
254 These associations were still significant after adjusting for the sex of the fetus and gestational weeks at
255 delivery, season of T1, and the gestational week at T1 (**Fig. 6b, Supplementary Data 10**). These
256 findings indicate that maternal vitamin D levels, especially in the second trimester, affect the immune cell
257 proportions in the babies at birth.

258 **DISCUSSION:**

259 In this study, we found that prenatal vitamin D deficiency by maternal dietary intervention reduced
260 peripheral T-cells in both the blood and spleen in adults and this reduction was linked to the decreased
261 number of bone marrow cells and the proportional alterations of hematopoietic progenitor cells in the
262 bone marrow. Our results demonstrate that cellular composition alterations could be the long-term
263 memories of prenatal exposure at the adult stage.

264 Besides insufficient nutritional intake or photosynthesis on the skin, genetic mutations
265 significantly contribute to vitamin D deficiency. In humans, mutations in genes of the vitamin D
266 biosynthetic pathway are the most common cause of heritable vitamin D-dependent rickets (VDDR),
267 which can be treated with active form vitamin D supplementation, whereas VDR mutation results in
268 hereditary vitamin D-resistant rickets (HVDR), which could partially be ameliorated with Ca2+
269 supplementation[67,68]. Animal models with gene knockout have been studied to understand the functions
270 of genes and diseases associated with them. A VDR Knockout mouse model study revealed that VDR
271 null mice are developed without any significant defects before birth; however, they developed a rickets-
272 like phenotype after weaning, and most of the animals died within 15 weeks after birth[40], suggesting VDR
273 is critical in the growth and bone formation in the post-weaning stage. Subsequent studies using the
274 same VDR knockout mouse line feeding normal chow diet identified that while VDR knockout mice
275 showed immune defects, no significant differences in the numbers or percentages of red and white cells
276 compared to their wildtype littermates were observed[36,37]. Interestingly, correcting hypocalcemia by
277 feeding a lactose-rich or polyunsaturated fat-rich diet was able to restore the immune abnormalities
278 observed in VDR knockout mice[37]. Another research group independently developed another VDR
279 knockout mouse line in C57BL/6 background and reported similar phenotypes, vitamin D-dependent
280 rickets type II with alopecia after weaning[42]. Studies using this mouse line revealed that this line also
281 developed immune abnormalities(39,69). Additionally, the nonobese diabetic (NOD) mouse line with a
282 VDR knockout showed that although diabetes onset is not accelerated by VDR deletion, NOD VDR
283 knockout mice develop rickets and have lower numbers of natural killer T-cells and CD4+CD25+ T-cells[41].

284 These findings from independent knockout mouse studies indicate that VDR-depleted animals are
285 phenotypically normal at birth but develop hypocalcemia within the first month of life and immune
286 abnormalities. The active form 1-α-25-dihydroxyvitamin D [1,25(OH)$_2$D] is synthesized from its precursor
287 25 hydroxyvitamin D [25(OH)D] via catalytic action of the 25(OH)D-1alpha-hydroxylase [1α(OH)ase]
288 enzyme, encoded by Cyp27b1. Mice deficient in 1α(OH)ase developed hypocalcemia, skeletal
289 abnormalities characteristics of rickets, female infertile, and a reduction in CD4 and CD8 peripheral T
290 lymphocytes after weaning[18]. A zebrafish study showed that loss of Cyp27b1-mediated biosynthesis by
291 gene knockdown significantly reduced *runx1* expression and hematopoietic stem and progenitor cell
292 productions[67]. In this study, we found that prenatal vitamin D deficiency-exposed offspring at the adult
293 stage did not show significant alterations in bone morphology, suggesting that vitamin D depletion during
294 development does not affect embryonic bone development and bone morphology later in life. On the
295 other hand, the immune phenotype of prenatal vitamin D deficiency-exposed offspring we observed was
296 much more severe than those of VDR knockout models and similar to the Cyp27b1 deletion models.
297 Since we observed this phenotype in offspring at 16 weeks of age, while VDR knockout mice typically do
298 not survive beyond 15 weeks[40], age might be another factor in developing this phenotype. However, our
299 findings suggest that the immune phenotypes in offspring exposed to prenatal vitamin D deficiency may
300 be caused by a lack of ligands rather than receptor malfunctions during the developmental phase.

301 A large biological difference between our study and the Cyp27b1 deletion models is the availability
302 of 1,25(OH)2D after weaning. All offspring were fed VDS diets after weaning, and the serum vitamin D
303 status of the VDD offspring became normal at five weeks of age. Therefore, the alterations we observed
304 at 16 weeks of age were not associated with the vitamin D deficiency status at the time of measurement.
305 However, it does indicate that prenatal vitamin D deficiency irreversibly alters bone marrow development
306 in the offspring. This aligns with a previous study conducted on rats[69]. The study found that the rats with
307 prenatal vitamin D deficiency by maternal dietary manipulation showed significant reductions in the total
308 number of nucleated bone marrow cells and in the colony-forming unit (CFU) content with a
309 corresponding increase in cell cycle rate[69]. The authors measured the CFU content by transplanting

310 nucleated bone marrow cells to AJ mice purchased from Jackson Laboratory (vitamin D-sufficient diet-
311 fed mice) and found that while 1,25(OH)2D3- or 24,25(OH)D3-treatment on vitamin D deficient rats in
312 postnatal life corrected the serum calcium and phosphate, the treatments did not reverse the CFU content
313 alterations. Their findings clearly demonstrate that prenatal and early-life vitamin D deficiency could
314 cause irreversible effects on HSC development. However, we cannot fully rule out the possibility that
315 alterations in hematopoietic stem cell niches might also be irreversibly altered. HSC niches in different
316 developmental stages play critical roles in the maintenance and differentiation of HSCs (reviewed by Gao
317 et al.[70]). It would be beneficial to explore this possibility further in upcoming research.

318 As a transcriptional regulation mechanism, 1,25(OH)2D binds to the VDR, which forms a
319 heterodimer with the retinoid X receptor and regulates gene expression by binding to vitamin D
320 responsive elements in genomic DNA. In this study, the transcription factor network analysis on e14.5
321 fetal liver scRNA-seq revealed that *Tal1*, *Lmo2*, *Runx1*, *Gata2, and Erg* downstream genes were
322 significantly enriched in VDD downregulated genes. We confirmed that the expressions of *Erg* and *Lmo2*
323 are regulated by VDR, as the treatment with 1-alpha-25-dihydroxyvitamin D3 (1,25$(OH)_2$D3) led to an
324 increase in gene expression in fetal hematopoietic progenitor cells, HPC7. A mutant and chimeric embryo
325 study reported that ERG is a direct upstream regulator of *Runx1* and *Gata2* in fetal livers[71], suggesting
326 prenatal vitamin D deficiency exposure perturbs the transcription profiles of the hematopoietic cells during
327 development via modulating hematopoiesis transcription factors regulated by VDR. Interestingly, this
328 transcription factor expression perturbation persists in the adult stage even though these mice were fed
329 a VDsuf diet and their vitamin D was fully recovered. Using bulk RNA-seq analysis, we identified 612
330 DEGs between VDD and VDS MPP4. Downregulated DEGs were enriched in hematopoietic-related
331 pathways, and many hematopoietic transcription factors, including *Tal1*, *Lmo2*, *Runx1*, *Gata1*, and Erg,
332 were downregulated. Gene Enrichment Analysis showed that the identified DEGs were enriched in the
333 DEGs of *Nfix* and *Srf* knockout mouse LSKs in the same direction. *Nfix* and *Srf* are hematopoietic
334 transcription factors. *Nfix* is associated with hematopoietic stem and progenitor cells (HSPCs) survival,
335 and *Srf* regulates hematopoietic stem cell adhesions. Although both *Nfix* and *Srf* were not identified as

336 DEGs, their expression levels were lower in VDD compared to VDS. It has been reported that loss of *Nfix*
337 expression in HSPCs of murine adult bone marrow is concomitant with the reduced expression of genes
338 associated with HSPCs survival, such as *Erg*, *Mecom*, and *Mpl* [52]. These same genes were also
339 significantly downregulated in VDD MPP4. However, the authors reported no selective loss of B, T, or
340 myeloid cells was observed in *Nfix*-depleted HSPCs [52]. On the other hand, Ragu *et al.* reported that
341 while depleting *Srf,* increased % of the LSK in the bone marrow, *Srf* knockout mice showed a significant
342 decline in white blood cell counts, which was primarily due to decreased numbers of circulating B and T
343 cells [53]. Our results suggest prenatal vitamin D deficiency modulates the *Nfix* and *Srf* pathways in the
344 long term.

345 Our study also revealed that higher maternal vitamin D levels during the second trimester were
346 associated with increased proportions of CD8+ T cells and decreased granulocytes in cord blood in
347 humans. The associations were maintained after adjusting for the season of the second trimester, the
348 gestational week at the maternal blood draw, the sex of the fetus, and the gestational week at birth.
349 Hematopoietic development consists of primitive and definitive hematopoiesis[72]. In mice, the definitive
350 hematopoiesis starts in the aorta-gonad mesonephros (AGM) region at approximately E10.5, then moves
351 to the liver around E12.5 and the bone marrow around E17.5 [73,74]. After birth, the bone marrow is the only
352 site where HSCs are maintained and expanded. In human development, the transition of the
353 hematopoietic stem cell production site from the fetal liver to bone marrow occurs in the second
354 trimester[74,75] when we observed significant associations. Recently, Elgormus et al. reported that newborn
355 serum vitamin D levels were negatively correlated with neutrophil-to-lymphocyte ratios (NLR) in newborn
356 babies[76]. The most common white blood cell is the granulocyte, composed of three distinct types:
357 neutrophils, eosinophils, and basophils. Among them, neutrophil is the most abundant type. Our results
358 and their finding concordantly indicate that the immune cell compositions, especially granulocyte
359 (neutrophil) and lymphocyte, of the babies are influenced by vitamin D levels in early life. Of note, cord
360 blood NLR has been proposed as an indicator for the diagnosis of early neonatal sepsis combined with
361 other laboratory tests and clinical manifestations[77–79]. The associations between neonatal sepsis and

362 cord blood vitamin D levels have been well reported. A meta-analysis of 18 studies revealed that low
363 maternal and cord blood vitamin D levels were significantly associated with the incidence of neonatal
364 sepsis[80]. Additionally, a study on 4,340 neonates appropriate for gestational age found a negative
365 correlation between cord blood NLR and fetal malnutrition. This indicates that cord blood NLR could be
366 utilized as a marker for fetal malnutrition[81]. Supplementing with Vitamin D during pregnancy may lower
367 the risks of neonatal sepsis and other adverse outcomes.

368 In conclusion, this study demonstrates that prenatal vitamin D deficiency reduces the number and
369 the proportion of MPP4 cells in the bone marrow, changing the expression status of the genes that may
370 be directly and indirectly regulated by VDR, and this alteration results in reduced T cell proportions in
371 peripheral blood and spleens of the offspring. The association between T cell proportion and maternal
372 vitamin D status was also observed in our BC-GENIST mother-baby cohorts. We and others have
373 reported that micronutrient deficiency changed the cellular compositions of adult mature organs and may
374 contribute to the phenotypes using animal dietary manipulation models[21,35,82]. These findings indicate that
375 the cell fate decision alteration of stem cells could be the key component of the long-term memory of
376 prenatal micronutrient deficiency, which links to disease risks later in life. Nevertheless, this study has
377 several limitations. A study conducted in Greece on mother-infant pairs revealed that insufficient levels
378 of vitamin D (<50 nmol/L) in pregnant mothers were linked to an increased occurrence of micronucleated
379 cells in binucleated T-cells[83]. Micronuclei are early indicators of genetic effects used to test the
380 relationship between exposure to genotoxic substances and cancer. However, our study did not explore
381 whether maternal VDD increases DNA damage risks in offspring. Sexual dimorphism is another covariate
382 we must explore. Since female mice did not show significant alterations in immune cell proportions in
383 adults, we only performed transcriptional analysis on male mice. Both males and females may have
384 prenatal and neonatal immune cell proportional alterations. Furthermore, there could be transcriptional
385 changes in certain genes in adult females, but these changes may not affect cell fate decisions. These
386 possibilities should be further investigated in future studies.

387

391 **METHODS:**

392 Maternal vitamin D deficiency mouse model

393 We purchased five-week-old C57BL/6J female mice from the Jackson Laboratory. After one week of
394 acclimation, we started dietary manipulations at six weeks old. Female mice (F0) were fed vitamin D
395 deficient (VDdef) or sufficient (VDsuf) diets for five weeks before mating with the control diet-fed male
396 mice and throughout the subsequent pregnancy. To avoid the paternal VDdef treatment effects, the
397 males did not stay in the female cage for more than three days. VDdef (0.0 IU/g vitamin D) and nutrient-
398 matched VDsuf (1.0 IU/g vitamin D) diets were obtained from Research Diets Inc. (10 kcal%fat, 20
399 kcal%Protein and 70 kcal%Carbonate). The detailed ingredients of each diet are listed in
400 **Supplementary Data 11**. VDdef-fed females were supplemented with 1.5% calcium gluconate water for
401 drinking water. After delivery, all F0 mice were fed VDsuf diets. The offspring were fed VDsuf diet after
402 weaning and maintained the diet until the sampling. All animal studies were approved by the Institutional
403 Animal Care and Use Committee at the Albert Einstein College of Medicine (protocol # 20160710).

404

405 Serum vitamin D level of mouse serum samples

406 Serum vitamin D (25(OH)D) levels of mouse serum samples were assessed by commercially available
407 ELISA kits (Eagle Biosciences, Inc. Amherst NH, or Abcam, Cambridge, MA) according to the
408 manufacturer's instructions. The signal was detected with BioTek Synergy 4 Microplate reader (Agilent
409 Technologies), and the results were analyzed using a 4-parameter logistic regression algorithm
410 (http://www.elisaanalysis.com/app). The measurements were performed as duplicates.

411

412 Immune cell profiling on peripheral blood and spleen

413 Immune cell profiling analysis was performed using flow cytometry (FACS Aria2, BD Biosciences) after
414 fluorescent dye conjugate antibodies staining. The obtained data were analyzed with FlowJo_10.6.1_CL
415 (https://www.flowjo.com/). Peripheral blood samples were collected using submandibular vein bleeding
416 methods. The spleen was obtained after euthanizing the animals with carbon dioxide inhalation. The

417 spleen samples were dissociated on 70 μm filters. The obtained single-cell suspensions were stained
418 with antibodies of immune cell surface marker proteins to identify cell types. Representative flow
419 cytometry traces are shown in **Supplementary Fig. 3.** The antibodies used in this study are listed in
420 **Supplementary Data 12**.
421
422 Isolating multipotent progenitor cells from bone marrow
423 Bone marrow cells were collected by crushing bones (tibia, Femur, iliac, sternum, and vertebrae). The
424 red cells were lysed with lysis buffer (150 mM $NH_4Cl$, 1 mM $KHCO_3$, and 0.1 mM EDTA). HSC/MPP
425 fractions were defined by the previously reported definition[50]. MPP4, lymphoid-primed hematopoietic
426 multipotent progenitor cells were isolated for gene expression analysis. Representative flow cytometry
427 traces are shown in **Supplementary Fig. 5.**
428
429 Cell culture
430 Hematopoietic progenitor cell line HPC-7 was kindly gifted by Dr. Britta Will at Albert Einstein College of
431 Medicine. HPC-7 cells were maintained at density of 1-10 $x10^5$/ml in Iscove's modified Dulbecco's
432 medium (Invitrogen) supplemented with 50-100 ng/ml of mouse stem cell factor (Gemini Bio-Products),
433 1 mM Sodium Pyruvate, 6.9 ng/mL α-Monothioglycerol (SIGMA-Aldrich), 5% of bovine calf serum and
434 Penicillin-Streptomycin. To examine the effect of vitamin D treatment on gene expression levels, the
435 HPC-7 cells were treated with 0.1 μM of 1alpha,25-Dihydroxyvitamin D3 (SIGMA-Aldrich) or 0.1%
436 (vol/vol) ethanol (solvent) for 24 hours.
437
438 RNA-seq library construction and sequencing
439 We performed RNA-seq on FACS isolate MPP4 cells (lymphoid primed-multipotent progenitor cells).
440 Total RNA was isolated with AllPrep DNA/RNA micro kit (QIAGEN). After we depleted ribosomal RNAs
441 from total RNA, we generated the RNA-seq libraries using KAPA RNA HyperPrep with RiboErase kit

442 (Roche). The generated libraries were sequenced on an Illumina NOVA-seq sequencer (Novogene Co.,
443 Ltd., USA).
444
445 RNA-seq alignment
446 After checking the quality of the sequencing files using FastQC[84] and trimming low-quality reads and
447 adapter sequences using Cutadapt[85], the obtained sequences were aligned to the mouse mm10
448 reference genome with the gencode M15 gene annotation using STAR aligner[86]. The quality of the library
449 was assessed with RSeQC[87]. The obtained transcript counts were analyzed with DESeq2. We identified
450 significant differentially expressed genes (DEGs) that showed two times higher or lower expression with
451 a false discovery rate-adjusted p-value less than 0.05. The detailed sequencing and alignment status are
452 listed in **Supplementary Data 1**.
453
454 Enrichment analysis for Gene Ontology (GO)
455 We used the Gene Ontology (GO) enrichment analyses and Gene Set Enrichment Analyses (GSEA) of
456 a Bioconductor package ClusterProfiler[88] to see the functional enrichment of DEGs. Q-values <0.05 were
457 considered significant.
458
459 Quantitative RT-PCR
460 Total RNA samples were isolated with AllPrep DNA/RNA micro kit, and cDNA libraries were synthesized
461 using SuperScript III transcriptase (Invitrogen) with random hexamer. The real-time PCR was performed
462 with Roche LightCycler 480 SYBR GREEN I Master mix on a LightCycler 480 system (Roche). Relative
463 gene expression abundance between samples was calculated using the CT method and *Gapdh* as an
464 internal control. The sequences of primers used in this study are listed in **Supplementary Data 13**.
465

466 Single-cell RNA sequencing library preparation

467 We used e14.5 male mouse liver (n=3 per group) to study transcriptional alteration at single-cell
468 resolution. The e14.5 mouse liver samples were dissociated on 70 μm filters, then each sample was
469 stained with unique cell hashing antibodies (BioLegend). 3,000-4,000 cells per sample were targeted
470 on the 10x Genomics Chromium platform. Single-cell mRNA libraries were built using the Chromium
471 Next GEM Single Cell 3' Library Construction V3 Kit, libraries sequenced on an Illumina NOVA-seq.
472 Sequencing data were aligned to mm10 mouse reference using the Cell Ranger 3.0.2 pipeline (10x
473 Genomics). Counting cell hashing tag were performed using CITE-seq Count version 1.3.4[89].

474

475 scRNA-seq data processing, batch correction, clustering, cell-type labeling, and data visualization

476 All scRNA-seq analysis and data visualization were performed using an R package, Seurat[54–56]. After
477 demultiplexing based on the cell hashing tag information, low-quality cells (<1000 genes/cell, <5000
478 reads/cell, and >10% mitochondrial reads/cell) were eliminated from the further analyses. Data
479 integration and identifying cell clusters were carried out after performing SCTransform[56]. Cell types of
480 each cell cluster were identified based on the expression of the marker genes[90]. Proportions of assigned
481 cell types were analyzed using Student's *t*-test. P-values <0.05 were considered significant. Differentially
482 expressed genes of each cell type between VDD and VDS were identified as at least 25% of cells
483 expressed the gene, the log fold change greater than 0.5, and the FDR adjusted p-value less than 0.05.
484 GO enrichment analysis was performed using a Bioconductor package ClusterProfiler[88] with q-values
485 <0.05 considered significant. The enrichment status of the transcription factors was assessed using the
486 CHEA transcription factor targets dataset[91] and TF Perturbations Followed by Expression functions
487 provided by Enrichr (http://amp.pharm.mssm.edu/Enrichr)[92].

488

489 Measurement of bone mineral density

490 Bone mineral density was measured humerus of the offspring at dissection. After the dissection, the left
491 arms (n=5-6 animals for each group) were scanned using an X-ray CT system, Inveon Multimodality
492 scanner (Siemens). The CT x-rays were generated by an 80kV peak voltage difference between the
493 cathode and tungsten target at 0.5 mA current and 200 millisecond exposure time. The arm samples
494 were placed on the 38mm width bed tandemly. The CT field of view was 5.5 cm by 8.5 cm with an overall
495 resolution without magnification of 60 microns. A Scout View was performed before the start of the CT
496 Acquisition to ensure the correct positioning of the subject in the field of view. Image analysis was
497 performed using MicroView (https://microview.parallax-innovations.com/).
498
499 Serum vitamin D level of serum samples from pregnant women
500 Healthy pregnant women were recruited as participants in The Birth Cohort Gene and Environment
501 Interaction Study of TMDU (BC-GENIST) project at the Tokyo Medical and Dental University, Bunkyo,
502 Tokyo, Japan[59,60]. Written informed consent was obtained from the participants, and the study was
503 approved by the Institutional Review Board of Tokyo Medical and Dental University (No. G2000-181, 29
504 July 2014). In this study, all participants were healthy Japanese females aged 27-42 years old without
505 smoking or drinking alcohol during their pregnancy. We used the following demographic information of
506 the participants in this study; maternal age at delivery, prepregnant body mass index, prenatal vitamin
507 supplements usage, sex of the fetus, gestation weeks, and estimated daily vitamin D intake. The daily
508 vitamin D intake was estimated 3-day food record questionnaire. Maternal serum samples were collected
509 twice, around 20 and 36 gestational weeks, and aliquoted samples were stored at -150 °C until use.
510 Serum 25(OH)$D_3$ levels were measured using a modified LC-APCI-MS/MS method[93]. As previously
511 described, this method involves the use of deuterated 25(OH)$D_3$ ($d_6$-25(OH)$D_3$) as an internal standard
512 compound and the selection of a precursor and product ion with an MS/MS multiple reaction monitoring
513 (MRM) method. The internal standard $d_6$-25(OH)$D_3$ (0.5 ng/10 μL) was added to serum (40 μL) and
514 precipitated with acetonitrile (200 μL). After evaporation of the supernatant, the precipitant was dissolved

515 with ethyl acetate (400 μL) and distilled water (200 μL) with vigorous shaking. The ethyl acetate phase
516 was removed and evaporated. Extracted vitamin D metabolites from serum were derivatized by 4-[2-(6,7-
517 dimethoxy-4-methyl-3-oxo-3,4-dihydroquinoxalyl)ethyl]-1,2,4-triazoline-3,5-dione (DMEQ-TAD) to obtain
518 high sensitivity by increasing ionization efficiency[94]. Separation was carried out using a reverse-phase
519 $C_{18}$ analytical column (CAPCELL PAK $C_{18}$ UG120, 5 μm; (4.6 I.D. × 250 mm) (SHISEIDO, Tokyo, Japan)
520 with a solvent system consisting of (A) acetonitrile, (B) distilled water (0–5 min A = 30%, 5–34 min
521 (A) = 30 → 70%, and 34–37 min (A) = 70 → 100%) as the mobile phase and a flow rate of 1.0 mL/min. All
522 MS data were collected in the positive ion mode, and quantitative analysis was carried out using MS/MS-
523 MRM of the precursor/product ion for DMED-TAQ-25(OH)$D_3$ (m/z; 746.5/468.1) and DMED-TAQ-$d_6$-
524 25(OH)$D_3$ (m/z; 752.5/468.1) with a dwell time of 200 ms (AB Sciex LLC., Framingham, MA, USA).
525
526 Estimation of immune cell profiles of human cord blood
527 We used a modified deconvolution approach to estimate the immune cell profiles of human cord blood
528 from the bulk DNA methylation profiles[95]. Bulk DNA methylation profiles of cord blood were accessed
529 using Infinium HumanMethylation450 BeadChip, and the estimation was performed using a Bioconductor
530 package FlowSorted.CordBloodCombined.450k[61].
531
532 Statistical analysis
533 Mouse phenotype results were analyzed using Student's *t*-test. The associations between maternal
534 serum vitamin D levels and immune cell profiles in human cord blood were tested using one-way
535 ANOVA. P-values <0.05 were considered significant. Differences in gene expression between VDD-F1
536 and VDS-F1 in RNA-seq were analyzed using DESeq2 with FDR-adjusted p-value <0.05. R v4.0
537 (https://www.r-project.org/) was used for most of the analyses.
538

539 **Table 1: Demographic information of BC-GENIST cohort**

| Total N (%) | | 74 (100.0) |
|---|---|---|
| Maternal age (yr) | Mean (SD) | 34.2 (4.0) |
| Pre-pregnancy BMI | Mean (SD) | 20.7 (2.6) |
| Prenatal vitamin usage, N (%) | Yes | 52 (70.3) |
| Fetal sex, N (%) | Female | 40 (54.1) |
| Gestational age at delivery (weeks) | Mean (SD) | 39.1 (1.2) |
| Gestational age at T1 | Mean (SD) | 19.0 (4.5) |
| Serum vitamin D concentration (ng/ml) at T1 | Mean (SD) | 25.2 (11.8) |
| Gestational age at T2 | Mean (SD) | 35.9 (0.9) |
| Serum vitamin D concentration (ng/ml) at T2 | Mean (SD) | 28.0 (14.4) |
| Estimated dietary vitamin D intake per day | Mean (SD) | 5.1 (4.4) |
| Maternal serum vitamin D deficiency levels, N(%) † | Deficient | 8 (10.8) |
| | Insufficient | 20 (27.0) |
| | Sufficient | 46 (62.2) |
| Estimated immune proportions from cord blood DNA methylation profiles | | |
| CD8 T cell | Mean (SD) | 5.23(3.35) |
| CD4 T cell | Mean (SD) | 19.25(7.15) |
| NK cell | Mean (SD) | 0.71(1.24) |
| B cell | Mean (SD) | 6.67(2.84) |
| Monocyte | Mean (SD) | 3.15(2.27) |
| Granulocyte | Mean (SD) | 61.46(9.2) |
| Nucleated red blood cell (nRBC) | Mean (SD) | 4.09(3.26) |

540
541
542 †: Deficient, both T1 and T2 serum vitamin D concentrations were less than 20 ng/ml; insufficient, one
543 of the measurements was less than 20 ng/ml and the other was less than 30 ng/ml
544
545

546 **FIGURE LEGENDS:**

547 **Fig.1: Study design**

548 Six-week-old female C57BL/6J mice were randomly assigned to the VDsuf or VDdef diet and fed the
549 assigned diet for five weeks before mating with a control diet-fed male. 1.5% calcium gluconate water
550 was supplemented to VDdef diet-fed group. After delivery, all F0 mice were fed VDsuf diets. The offspring
551 were fed VDsuf diet after weaning and maintained the diet until the sampling.

552

553 **Fig.2: Prenatal vitamin D deficiency reduces CD4+ and CD8+ T cells in the periphery at the adult**
554 **stage.**

555 T cell proportions in the peripheral blood (**a**) and spleen (**b**) were significantly decreased in VDD offspring.
556 Each dot on the plot represents a sample (blood, n=11 per group; spleen, n=6 per group). The box shows
557 the range between the first and third quartiles. The upper and lower whiskers represent 1.5 times the
558 interquartile range, while the black bars indicate the median. The values shown in the plot are p-values
559 calculated using Student's t-test.

560

561 **Fig.3: Prenatal vitamin D deficiency decreased the number of bone marrow cells and LSKs and**
562 **concomitantly reduced lymphoid lineage cells at the adult stage.**

563 Prenatal vitamin D deficiency reduced the total number of bone marrow cells (n=9 for VDD and n=10 for
564 VDS) (**a**) and the number of LSKs in bone marrow (n=9 per group) (**b**). The differences in total HSC,
565 long-term and short-term HSC, and three MPPs in the bone marrow (n=9 for VDD and n=10 for VDS) (**c**)
566 and hematopoietic progenitor cells in the bone marrow (n=9 per group) of VDD and VDS mice are
567 displayed in the box plots (**d**). A significant decrease in MPP4, CLP, and Lin-/CD127+ cells was observed
568 in VDD mice, indicating that prenatal vitamin D deficiency disproportionately affects the production of
569 hematopoietic lineages. Each dot on the plot represents a sample. The box shows the range between
570 the first and third quartiles. The upper and lower whiskers represent 1.5 times the interquartile range,

571 while the black bars indicate the median. The values shown in the plot are p-values calculated using
572 Student's t-test.
573
574 **Fig.4: Bulk RNA-seq analyses reveal the transcriptional alterations in MPP4.**
575 Bulk RNA-seq analysis identified significant differences in the transcriptional profiles of MPP4 between
576 VDD and VDS (n=3 per group). (a) The heatmap and dendrogram show a distinct clustering between
577 VDD and VDS. (**b**) The volcano plot displays the -log10 adjusted p-values and log2 fold-change
578 differences of the identified DEGs. Each dot represents a gene, and significant DEGs are indicated by
579 red dots. (**c**) The GO enrichment analysis reveals that the up-regulated DEGs between VDD and VDS
580 MPP4 are enriched in Leukocyte migration and chemotaxis-related genes. The dot plot shows the
581 significance and the gene ratios of the top eight GO terms (left), and the Cnet plot indicates the identified
582 DEGs of the top five GO terms (right). (**d**) The GO enrichment analysis reveals that the down-regulated
583 DEGs between VDD and VDS MPP4 are enriched in the regulation of hematopoiesis-related genes. The
584 dot plot shows the significance and the gene ratios of the top eight GO terms (left), and the Cnet plot
585 indicates the identified DEGs of the top five GO terms (right).
586
587 **Fig. 5: Prenatal vitamin D deficiency alters cellular compositions of the embryonic liver,**
588 **suggesting immune cell proportion changes start during development.**
589 (**a**) UMAP representation of single-cell RNA-seq gene expression data and cellular lineage identification
590 of E14.5 fetal liver (n=3 per group). (**b**) The boxplots indicate prenatal vitamin D deficiency alters cellular
591 compositions of E14.5 fetal liver. (**c**) Genes downregulated in VDD E14.5 fetal liver are enriched in the
592 genes regulated by hematopoietic transcription factors. (**d**) Treating HPC7 cells with 1-alpha-25-
593 dihydroxyvitamin $D_3$ significantly increases gene expression levels of *Erg* and *Lmo2*, suggesting these
594 genes are regulated by VDR (n=3 per treatment group).
595

596 **Fig. 6: Maternal serum vitamin D status in the second trimester is positively associated with the**
597 **CD8+ T cell proportion in the cord blood.**
598 (**a**) The heatmap shows that the gestational week at the delivery has the strongest associations with
599 immune cell composition variations assessed by the principal component (PC), followed by maternal
600 serum vitamin D ($2^{nd}$ trimester) and being born in the summer season. (**b**) After adjusting for the sex of the
601 fetus, gestational age, the season of T1, and the gestational week at T1, maternal serum vitamin D ($2^{nd}$
602 trimester) maintains significant associations with immune cell composition, specifically positive association
603 with proportions of CD8+ T cell and monocytes, and negative association with granulocytes. Asterisks indicate
604 the significance (** $p<0.01$ and * $p<0.05$, Student's t-test). The left panel shows -log10(p-value), and the right
605 panel shows the direction of the associations.
606
607 **DESCRIPTION OF SUPPLEMENTARY INFORMATION:**
608 **Supplementary Fig. 1:** The effects of vitamin D deficient diet feeding on the mothers and the impacts of
609 prenatal VDD on the growth and bone density of offspring at the adult stage.
610 **Supplementary Fig. 2:** Prenatal VDD effects on female offspring at the adult stage.
611 **Supplementary Fig. 3:** Gating and analytical strategies to assess the immune cell profiles in peripheral
612 blood and spleen.
613 **Supplementary Fig. 4:** Prenatal vitamin D deficiency alters hematopoietic cell cellular compositions of
614 bone marrow at the adult stage.
615 **Supplementary Fig. 5:** Gating and analytical strategies to assess hematopoietic stem cells, multipotent
616 progenitor cells, and progenitor cells from bone marrow.
617 **Supplementary Fig. 6:** Differentially expressed genes (DEGs) in VDD MPP4 are enriched in DEGs of
618 hematopoietic transcription factor knockout models.
619 **Supplementary Fig. 7:** The heatmaps indicate the association between known covariates and immune
620 cell proportions.
621

622 **DESCRIPTION OF ADDITIONAL SUPPLEMENTARY INFORMATION**

623 **Supplementary Data 1:** RNA-seq sequencing stats (VDD and VDS MPP4)

624 **Supplementary Data 2:** A list of differentially expressed genes between VDD MPP4 and VDS MPP4

625 **Supplementary Data 3:** The results of GO enrichment analysis on MPP4 GEGs

626 **Supplementary Data 4:** The results of Gene Set Enrichment Analysis on MPP4 DEGs

627 **Supplementary Data 5:** A list of the marker genes of each cell cluster found in E14.5 fetal liver scRNAseq
628 analysis

629 **Supplementary Data 6:** A list of DEGs of each cell cluster found in E14.5 fetal liver scRNAseq analysis

630 **Supplementary Data 7:** A list of DEGs in pseudo bulk RNA-seq analysis of E14.5 fetal liver scRNAseq

631 **Supplementary Data 8:** The results of Enrichr analysis on differentially expressed genes identified in
632 pseudo bulk RNA-seq analysis of E14.5 fetal liver scRNAseq

633 **Supplementary Data 9:** Summary of the associations of known covariates to the maternal serum vitamin
634 D levels

635 **Supplementary Data 10:** A list of the significance of the contribution to the proportions

636 **Supplementary Data 11:** The detailed ingredients of each diet

637 **Supplementary Data 12:** A list of antibodies used in this study

638 **Supplementary Data 13:** A list of primer sequences used in this study

**DATA AVAILABILITY:**

The authors declare that all data supporting the findings of this study are available within the article and its supplementary information files, except for human cord blood analyses, which may contain sensitive information. All sequencing data, RNA-seq and scRNA-seq of this study, is deposited in NCBI's Gene Expression Omnibus GEO database under the accession number GSE242043, and processed data and code used in this study are available upon request.

**ACKNOWLEDGMENTS:**

The authors thank Dr. Britta Will at Albert Einstein College of Medicine for generously providing the HPC7 cells. Additionally, we would like to acknowledge the MicroPET Facility, supported by The M. Donald Blaufox Laboratory for Molecular Imaging and NIH (1S10RR029545" MicroPET/SPECT/CT Animal Imaging Device"), the Flow Cytometry Core Facility, and the Genomic Core Facility at Albert Einstein College of Medicine.

**FUNDING:**

This work was supported by the Human Genomic Pilot Grant; Department of Genetics, Albert Einstein College of Medicine (M.S.), internal Texas A&M AgriLife Research (M.S.), the National Institutes of Health under award number R01HL145302 (M.S.) and R01DK136989 (M.S.), Nanken-Kyoten, Tokyo Medical and Dental University, under award number 2021-kokusai 02 (M.S.), and Mishima Kaiun Memorial Fund (M.S.). This work was also supported by Jane A. and Myles P. Dempsey and by NIH grant R35CA253127 (to U.G.S.). U.G.S. holds the Edward P. Evans Endowed Professorship in Myelodysplastic Syndromes at Albert Einstein College of Medicine. The Endowed Professorship was supported by a grant from the Edward P. Evans Foundation.

The content is solely the responsibility of the authors and does not necessarily represent the official views of the National Institutes of Health.

**AUTHOR INFORMATION:**

**Authors and Affiliations**

These authors contributed equally: Koki Ueda, Shu Shien Chin, Noriko Sato

**Department of Cell Biology, Albert Einstein College of Medicine, Bronx, NY, USA**

Koki Ueda, Ulrich G. Steidl

**Department of Blood Transfusion and Transplantation Immunology, Fukushima Medical University, Fukushima, Fukushima, Japan**

Koki Ueda

**Department of Food and Nutrition, Faculty of Human Sciences and Design, Japan Women's University, Bunkyo-ku, Tokyo, Japan**

Noriko Sato

**Department of Microbiology & Immunology, Albert Einstein College of Medicine, Bronx, NY, USA**

Shu Shien Chin, Laurent Chorro, Gregoire Lauvau

**Graduate School of Medical and Dental Sciences, Medical and Dental Sciences, Systemic Organ Regulation, Comprehensive Reproductive Medicine Tokyo Medical and Dental University, Bunkyo-ku, Tokyo**

Naoyuki Miyasaka

**Department of Genetics, Albert Einstein College of Medicine, Bronx, NY, USA**

Betelehem Solomon Bera, David Reynolds, Reanna Doña-Termine, John M. Greally, Masako Suzuki

**Department of Biotechnology, Faculty of Engineering, Toyama Prefectural University, Toyama, Japan**

Miyu Nishikawa

**Department of Pharmaceutical Engineering, Faculty of Engineering, Toyama Prefectural University, Toyama, Japan**

Kaori Yasuda

**Department of Radiology, Albert Einstein College of Medicine, Bronx, NY, USA**

691 Wade R Koba

692 **Ruth L. and David S. Gottesman Institute for Stem Cell Research and Regenerative Medicine,**

693 **Albert Einstein College of Medicine, Bronx, NY 10461, USA**

694 Ulrich G. Steidl

695 **Department of Oncology, Albert Einstein College of Medicine – Montefiore Medical Center,**

696 **Bronx, NY 10461, USA**

697 Ulrich G. Steidl

698 **Department of Pediatrics, Albert Einstein College of Medicine – Montefiore Medical Center,**

699 **Bronx, NY 10461, USA**

700 John M. Greally

701 **Montefiore-Einstein Cancer Center, Albert Einstein College of Medicine – Montefiore Medical**

702 **Center, Bronx, NY 10461, USA**

703 Ulrich G. Steidl

704 **Department of Nutrition, Texas A&M University, College Station, TX, USA**

705 Masako Suzuki

706

707 **Contributions**

708 Conceptualization and methodology, G.L., U.G.S, J.M.G., and M.S.; investigation, K.U., N.S.,

709 S.S.C., M.N., K.Y., B.S.B., L.C., R.D.T., W.R.K., D.R., and M.S.; formal analysis and software,

710 K.U., N.S., S.S.C., M.N., K.Y., and M.S.; resources, N.M. and N.S.; writing—original draft,

711 M.S.; writing—review and editing, all authors. Supervision, G.L., U.G.S, J.M.G., and M.S.

712

713 **Corresponding authors**

714 Correspondence to Masako Suzuki.

715

716 **ETHICS DECLARATIONS:**

717 **Competing interests**

718 The authors declare no competing interests.

719

720

721 **REFERENCE**


722 1. Mostafa, W.Z., and Hegazy, R.A. (2015). Vitamin D and the skin: Focus on a complex
723 relationship: A review. J. Advanc. Res. *6*, 793–804. 10.1016/j.jare.2014.01.011.

724 2. Bodnar, L.M., Catov, J.M., Simhan, H.N., Holick, M.F., Powers, R.W., and Roberts, J.M. (2007).
725 Maternal vitamin D deficiency increases the risk of preeclampsia. J. Clin. Endocrinol. Metab. *92*,
726 3517–3522. 10.1210/jc.2007-0718.

727 3. van der Pligt, P., Willcox, J., Szymlek-Gay, E.A., Murray, E., Worsley, A., and Daly, R.M. (2018).
728 Associations of Maternal Vitamin D Deficiency with Pregnancy and Neonatal Complications in
729 Developing Countries: A Systematic Review. Nutrients *10*. 10.3390/nu10050640.

730 4. Zosky, G.R., Hart, P.H., Whitehouse, A.J.O., Kusel, M.M., Ang, W., Foong, R.E., Chen, L., Holt,
731 P.G., Sly, P.D., and Hall, G.L. (2014). Vitamin D deficiency at 16 to 20 weeks' gestation is
732 associated with impaired lung function and asthma at 6 years of age. Ann. Am. Thorac. Soc. *11*,
733 571–577. 10.1513/AnnalsATS.201312-423OC.

734 5. Weinert, L.S., and Silveiro, S.P. (2015). Maternal-fetal impact of vitamin D deficiency: a critical
735 review. Matern. Child Health J. *19*, 94–101. 10.1007/s10995-014-1499-7.

736 6. Hart, P.H., Lucas, R.M., Walsh, J.P., Zosky, G.R., Whitehouse, A.J.O., Zhu, K., Allen, K.L.,
737 Kusel, M.M., Anderson, D., and Mountain, J.A. (2015). Vitamin D in fetal development: findings
738 from a birth cohort study. Pediatrics *135*, e167-73. 10.1542/peds.2014-1860.

739 7. Gilani, S., and Janssen, P. (2019). Maternal Vitamin D Levels During Pregnancy and Their
740 Effects on Maternal-Fetal Outcomes: A Systematic Review. J. Obstet. Gynaecol. Can.
741 10.1016/j.jogc.2019.09.013.

742 8. Cashman, K.D. (2018). Vitamin D Requirements for the Future-Lessons Learned and Charting a
743 Path Forward. Nutrients *10*. 10.3390/nu10050533.

744 9. Roth, D.E., Morris, S.K., Zlotkin, S., Gernand, A.D., Ahmed, T., Shanta, S.S., Papp, E., Korsiak,
745 J., Shi, J., Islam, M.M., et al. (2018). Vitamin D supplementation in pregnancy and lactation and
746 infant growth. N. Engl. J. Med. *379*, 535–546. 10.1056/NEJMoa1800927.

747 10. Cashman, K.D. (2020). Vitamin D deficiency: defining, prevalence, causes, and strategies of
748 addressing. Calcif. Tissue Int. *106*, 14–29. 10.1007/s00223-019-00559-4.

749 11. Aspelund, T., Grübler, M.R., Smith, A.V., Gudmundsson, E.F., Keppel, M., Cotch, M.F., Harris,
750 T.B., Jorde, R., Grimnes, G., Joakimsen, R., et al. (2019). Effect of Genetically Low 25-
751 Hydroxyvitamin D on Mortality Risk: Mendelian Randomization Analysis in 3 Large European
752 Cohorts. Nutrients *11*. 10.3390/nu11010074.

753 12. Forrest, K.Y.Z., and Stuhldreher, W.L. (2011). Prevalence and correlates of vitamin D deficiency
754 in US adults. Nutr. Res. *31*, 48–54. 10.1016/j.nutres.2010.12.001.

755 13. Liu, X., Baylin, A., and Levy, P.D. (2018). Vitamin D deficiency and insufficiency among US
756 adults: prevalence, predictors and clinical implications. Br. J. Nutr. *119*, 928–936.
757 10.1017/S0007114518000491.

758 14. Lips, P. (2010). Worldwide status of vitamin D nutrition. J. Steroid Biochem. Mol. Biol. *121*, 297–
759 300. 10.1016/j.jsbmb.2010.02.021.

760 15. Holick, M.F. (2006). Resurrection of vitamin D deficiency and rickets. J. Clin. Invest. *116*, 2062–
761 2072. 10.1172/JCI29449.

762 16. Pike, J.W., Meyer, M.B., Lee, S.-M., Onal, M., and Benkusky, N.A. (2017). The vitamin D
763 receptor: contemporary genomic approaches reveal new basic and translational insights. J. Clin.
764 Invest. *127*, 1146–1154. 10.1172/JCI88887.

765 17. Yetgin, S., and Ozsoylu, S. (1982). Myeloid metaplasia in vitamin D deficiency rickets. Scand. J.
766 Haematol. *28*, 180–185. 10.1111/j.1600-0609.1982.tb00512.x.

767 18. Panda, D.K., Miao, D., Tremblay, M.L., Sirois, J., Farookhi, R., Hendy, G.N., and Goltzman, D.
768 (2001). Targeted ablation of the 25-hydroxyvitamin D 1alpha -hydroxylase enzyme: evidence for
769 skeletal, reproductive, and immune dysfunction. Proc Natl Acad Sci USA *98*, 7498–7503.
770 10.1073/pnas.131029498.

771 19. Maka, N., Makrakis, J., Parkington, H.C., Tare, M., Morley, R., and Black, M.J. (2008). Vitamin
772 D deficiency during pregnancy and lactation stimulates nephrogenesis in rat offspring. Pediatr.
773 Nephrol. *23*, 55–61. 10.1007/s00467-007-0641-9.

774 20. Gezmish, O., and Black, M.J. (2013). Vitamin D deficiency in early life and the potential
775 programming of cardiovascular disease in adulthood. J. Cardiovasc. Transl. Res. *6*, 588–603.
776 10.1007/s12265-013-9475-y.

777 21. Foong, R.E., Bosco, A., Jones, A.C., Gout, A., Gorman, S., Hart, P.H., and Zosky, G.R. (2015).
778 The effects of in utero vitamin D deficiency on airway smooth muscle mass and lung function.
779 Am. J. Respir. Cell Mol. Biol. *53*, 664–675. 10.1165/rcmb.2014-0356OC.

780 22. Hawes, J.E., Tesic, D., Whitehouse, A.J., Zosky, G.R., Smith, J.T., and Wyrwoll, C.S. (2015).
781 Maternal vitamin D deficiency alters fetal brain development in the BALB/c mouse. Behav. Brain
782 Res. *286*, 192–200. 10.1016/j.bbr.2015.03.008.

783 23. Wu, J., Zhong, Y., Shen, X., Yang, K., and Cai, W. (2018). Maternal and early-life vitamin D
784 deficiency enhances allergic reaction in an ovalbumin-sensitized BALB/c mouse model. Food
785 Nutr. Res. *62*. 10.29219/fnr.v62.1401.

786 24. Belenchia, A.M., Johnson, S.A., Ellersieck, M.R., Rosenfeld, C.S., and Peterson, C.A. (2017). In
787 utero vitamin D deficiency predisposes offspring to long-term adverse adipose tissue effects. J.
788 Endocrinol. *234*, 301–313. 10.1530/JOE-17-0015.

789 25. Belenchia, A.M., Jones, K.L., Will, M., Beversdorf, D.Q., Vieira-Potter, V., Rosenfeld, C.S., and
790 Peterson, C.A. (2018). Maternal vitamin D deficiency during pregnancy affects expression of
791 adipogenic-regulating genes peroxisome proliferator-activated receptor gamma (PPARγ) and
792 vitamin D receptor (VDR) in lean male mice offspring. Eur. J. Nutr. *57*, 723–730.
793 10.1007/s00394-016-1359-x.

794 26. Reichetzeder, C., Chen, H., Föller, M., Slowinski, T., Li, J., Chen, Y.-P., Lang, F., and Hocher,
795 B. (2014). Maternal vitamin D deficiency and fetal programming--lessons learned from humans
796 and mice. Kidney Blood Press. Res. *39*, 315–329. 10.1159/000355809.

797 27. Nicholas, C., Davis, J., Fisher, T., Segal, T., Petti, M., Sun, Y., Wolfe, A., and Neal-Perry, G.
798 (2016). Maternal vitamin D deficiency programs reproductive dysfunction in female mice
799 offspring through adverse effects on the neuroendocrine axis. Endocrinology *157*, 1535–1545.
800 10.1210/en.2015-1638.

801 28. Liu, N.Q., Ouyang, Y., Bulut, Y., Lagishetty, V., Chan, S.Y., Hollis, B.W., Wagner, C., Equils, O.,
802 and Hewison, M. (2013). Dietary vitamin D restriction in pregnant female mice is associated with
803 maternal hypertension and altered placental and fetal development. Endocrinology *154*, 2270–
804 2280. 10.1210/en.2012-2270.

805 29. Xue, J., Schoenrock, S.A., Valdar, W., Tarantino, L.M., and Ideraabdullah, F.Y. (2016). Maternal
806 vitamin D depletion alters DNA methylation at imprinted loci in multiple generations. Clin.
807 Epigenetics *8*, 107. 10.1186/s13148-016-0276-4.

808 30. Fernandes de Abreu, D.A., Landel, V., Barnett, A.G., McGrath, J., Eyles, D., and Feron, F.
809 (2012). Prenatal vitamin D deficiency induces an early and more severe experimental
810 autoimmune encephalomyelitis in the second generation. Int. J. Mol. Sci. *13*, 10911–10919.
811 10.3390/ijms130910911.

812 31. Maia-Ceciliano, T.C., Barreto-Vianna, A.R.C., Barbosa-da-Silva, S., Aguila, M.B., Faria, T.S.,
813 and Mandarim-de-Lacerda, C.A. (2016). Maternal vitamin D-restricted diet has consequences in
814 the formation of pancreatic islet/insulin-signaling in the adult offspring of mice. Endocrine *54*, 60–
815 69. 10.1007/s12020-016-0973-y.

816 32. Nascimento, F.A.M., Ceciliano, T.C., Aguila, M.B., and Mandarim-de-Lacerda, C.A. (2012).
817 Maternal vitamin D deficiency delays glomerular maturity in F1 and F2 offspring. PLoS ONE *7*,
818 e41740. 10.1371/journal.pone.0041740.

819 33. Nascimento, F.A.M., Ceciliano, T.C., Aguila, M.B., and Mandarim-de-Lacerda, C.A. (2013).
820 Transgenerational effects on the liver and pancreas resulting from maternal vitamin D restriction
821 in mice. J. Nutr. Sci. Vitaminol. *59*, 367–374. 10.3177/jnsv.59.367.

822 34. Liang, Y., Yu, H., Ke, X., Eyles, D., Sun, R., Wang, Z., Huang, S., Lin, L., McGrath, J.J., Lu, J.,
823 et al. (2020). Vitamin D deficiency worsens maternal diabetes induced neurodevelopmental
824 disorder by potentiating hyperglycemia-mediated epigenetic changes. Ann. N. Y. Acad. Sci.
825 10.1111/nyas.14535.

826 35. Lundy, K., Greally, J.F., Essilfie-Bondzie, G., Olivier, J.B., Doña-Termine, R., Greally, J.M., and
827 Suzuki, M. (2022). Vitamin D deficiency during development permanently alters liver cell
828 composition and function. Front Endocrinol (Lausanne) *13*, 860286.
829 10.3389/fendo.2022.860286.

830 36. O'Kelly, J., Hisatake, J., Hisatake, Y., Bishop, J., Norman, A., and Koeffler, H.P. (2002). Normal
831 myelopoiesis but abnormal T lymphocyte responses in vitamin D receptor knockout mice. J. Clin.
832 Invest. *109*, 1091–1099. 10.1172/JCI12392.

833 37. Mathieu, C., Van Etten, E., Gysemans, C., Decallonne, B., Kato, S., Laureys, J., Depovere, J.,
834 Valckx, D., Verstuyf, A., and Bouillon, R. (2001). In vitro and in vivo analysis of the immune
835 system of vitamin D receptor knockout mice. J. Bone Miner. Res. *16*, 2057–2065.
836 10.1359/jbmr.2001.16.11.2057.

837 38. Yu, S., and Cantorna, M.T. (2011). Epigenetic reduction in invariant NKT cells following in utero
838 vitamin D deficiency in mice. J. Immunol. *186*, 1384–1390. 10.4049/jimmunol.1002545.

839 39. Yu, S., and Cantorna, M.T. (2008). The vitamin D receptor is required for iNKT cell
840 development. Proc Natl Acad Sci USA *105*, 5207–5212. 10.1073/pnas.0711558105.

841 40. Yoshizawa, T., Handa, Y., Uematsu, Y., Takeda, S., Sekine, K., Yoshihara, Y., Kawakami, T.,
842 Arioka, K., Sato, H., Uchiyama, Y., et al. (1997). Mice lacking the vitamin D receptor exhibit
843 impaired bone formation, uterine hypoplasia and growth retardation after weaning. Nat. Genet.
844 *16*, 391–396. 10.1038/ng0897-391.

845 41. Gysemans, C., van Etten, E., Overbergh, L., Giulietti, A., Eelen, G., Waer, M., Verstuyf, A.,
846 Bouillon, R., and Mathieu, C. (2008). Unaltered diabetes presentation in NOD mice lacking the
847 vitamin D receptor. Diabetes *57*, 269–275. 10.2337/db07-1095.

848 42. Li, Y.C., Pirro, A.E., Amling, M., Delling, G., Baron, R., Bronson, R., and Demay, M.B. (1997).
849 Targeted ablation of the vitamin D receptor: an animal model of vitamin D-dependent rickets type
850 II with alopecia. Proc Natl Acad Sci USA *94*, 9831–9835.

851 43. Camargo, C.A., Rifas-Shiman, S.L., Litonjua, A.A., Rich-Edwards, J.W., Weiss, S.T., Gold, D.R.,
852 Kleinman, K., and Gillman, M.W. (2007). Maternal intake of vitamin D during pregnancy and risk
853 of recurrent wheeze in children at 3 y of age. Am. J. Clin. Nutr. *85*, 788–795.
854 10.1093/ajcn/85.3.788.

855 44. Brehm, J.M., Schuemann, B., Fuhlbrigge, A.L., Hollis, B.W., Strunk, R.C., Zeiger, R.S., Weiss,
856 S.T., Litonjua, A.A., and Childhood Asthma Management Program Research Group (2010).
857 Serum vitamin D levels and severe asthma exacerbations in the Childhood Asthma Management
858 Program study. J. Allergy Clin. Immunol. *126*, 52-8.e5. 10.1016/j.jaci.2010.03.043.

859 45. Mirzaei, F., Michels, K.B., Munger, K., O'Reilly, E., Chitnis, T., Forman, M.R., Giovannucci, E.,
860 Rosner, B., and Ascherio, A. (2011). Gestational vitamin D and the risk of multiple sclerosis in
861 offspring. Ann. Neurol. *70*, 30–40. 10.1002/ana.22456.

862 46. Mulligan, M.L., Felton, S.K., Riek, A.E., and Bernal-Mizrachi, C. (2010). Implications of vitamin D
863 deficiency in pregnancy and lactation. Am. J. Obstet. Gynecol. *202*, 429.e1-9.
864 10.1016/j.ajog.2009.09.002.

865 47. Stene, L.C., Ulriksen, J., Magnus, P., and Joner, G. (2000). Use of cod liver oil during
866 pregnancy associated with lower risk of Type I diabetes in the offspring. Diabetologia *43*, 1093–
867 1098. 10.1007/s001250051499.

868 48. Vitamin D supplement in early childhood and risk for Type I (insulin-dependent) diabetes
869 mellitus. The EURODIAB Substudy 2 Study Group. (1999). Diabetologia *42*, 51–54.
870 10.1007/s001250051112.

871 49. Seipelt, E.M., Tourniaire, F., Couturier, C., Astier, J., Loriod, B., Vachon, H., Pucéat, M.,
872 Mounien, L., and Landrier, J.-F. (2020). Prenatal maternal vitamin D deficiency sex-dependently
873 programs adipose tissue metabolism and energy homeostasis in offspring. FASEB J. *34*, 14905–
874 14919. 10.1096/fj.201902924RR.

875 50. Pietras, E.M., Reynaud, D., Kang, Y.-A., Carlin, D., Calero-Nieto, F.J., Leavitt, A.D., Stuart, J.M.,
876 Göttgens, B., and Passegué, E. (2015). Functionally Distinct Subsets of Lineage-Biased
877 Multipotent Progenitors Control Blood Production in Normal and Regenerative Conditions. Cell
878 Stem Cell *17*, 35–46. 10.1016/j.stem.2015.05.003.

879 51. Challen, G.A., Boles, N., Lin, K.K.-Y., and Goodell, M.A. (2009). Mouse hematopoietic stem cell
880 identification and analysis. Cytometry A *75*, 14–24. 10.1002/cyto.a.20674.

881 52. Holmfeldt, P., Pardieck, J., Saulsberry, A.C., Nandakumar, S.K., Finkelstein, D., Gray, J.T.,
882 Persons, D.A., and McKinney-Freeman, S. (2013). Nfix is a novel regulator of murine
883 hematopoietic stem and progenitor cell survival. Blood *122*, 2987–2996. 10.1182/blood-2013-04-
884 493973.

885 53. Ragu, C., Elain, G., Mylonas, E., Ottolenghi, C., Cagnard, N., Daegelen, D., Passegué, E.,
886 Vainchenker, W., Bernard, O.A., and Penard-Lacronique, V. (2010). The transcription factor Srf
887 regulates hematopoietic stem cell adhesion. Blood *116*, 4464–4473. 10.1182/blood-2009-11-
888 251587.

889 54. Satija, R., Farrell, J.A., Gennert, D., Schier, A.F., and Regev, A. (2015). Spatial reconstruction of
890 single-cell gene expression data. Nat. Biotechnol. *33*, 495–502. 10.1038/nbt.3192.

891 55. Butler, A., Hoffman, P., Smibert, P., Papalexi, E., and Satija, R. (2018). Integrating single-cell
892 transcriptomic data across different conditions, technologies, and species. Nat. Biotechnol. *36*,
893 411–420. 10.1038/nbt.4096.

894 56. Hafemeister, C., and Satija, R. (2019). Normalization and variance stabilization of single-cell
895 RNA-seq data using regularized negative binomial regression. Genome Biol. *20*, 296.
896 10.1186/s13059-019-1874-1.

897 57. Wang, X., Yang, L., Wang, Y.-C., Xu, Z.-R., Feng, Y., Zhang, J., Wang, Y., and Xu, C.-R.
898 (2020). Comparative analysis of cell lineage differentiation during hepatogenesis in humans and
899 mice at the single-cell transcriptome level. Cell Res. *30*, 1109–1126. 10.1038/s41422-020-0378-
900 6.

901 58. Pinto do O, P., Kolterud, A., and Carlsson, L. (1998). Expression of the LIM-homeobox gene
902 LH2 generates immortalized steel factor-dependent multipotent hematopoietic precursors.
903 EMBO J. *17*, 5744–5756. 10.1093/emboj/17.19.5744.

904 59. Pavethynath, S., Imai, C., Jin, X., Hichiwa, N., Takimoto, H., Okamitsu, M., Tarui, I., Aoyama, T.,
905 Yago, S., Fudono, A., et al. (2019). Metabolic and Immunological Shifts during Mid-to-Late
906 Gestation Influence Maternal Blood Methylation of CPT1A and SREBF1. Int. J. Mol. Sci. *20*.
907 10.3390/ijms20051066.

908 60. Sato, N., Fudono, A., Imai, C., Takimoto, H., Tarui, I., Aoyama, T., Yago, S., Okamitsu, M.,
909 Mizutani, S., and Miyasaka, N. (2021). Placenta mediates the effect of maternal hypertension
910 polygenic score on offspring birth weight: a study of birth cohort with fetal growth velocity data.
911 BMC Med. *19*, 260. 10.1186/s12916-021-02131-0.

912 61. Lucas A., K.G., Meaghan C.,. Kelly M.,. Devin C.,. John K.,. Karl T.,. Robert Lyle, Brock C.,.
913 Janine Felix (2019). FlowSorted.CordBloodCombined.450k. Bioconductor.
914 10.18129/b9.bioc.flowsorted.cordbloodcombined.450k.

915 62. Gervin, K., Salas, L.A., Bakulski, K.M., van Zelm, M.C., Koestler, D.C., Wiencke, J.K., Duijts, L.,
916 Moll, H.A., Kelsey, K.T., Kobor, M.S., et al. (2019). Systematic evaluation and validation of
917 reference and library selection methods for deconvolution of cord blood DNA methylation data.
918 Clin. Epigenetics *11*, 125. 10.1186/s13148-019-0717-y.

919 63. Salas, L.A., Koestler, D.C., Butler, R.A., Hansen, H.M., Wiencke, J.K., Kelsey, K.T., and
920 Christensen, B.C. (2018). An optimized library for reference-based deconvolution of whole-blood
921 biospecimens assayed using the Illumina HumanMethylationEPIC BeadArray. Genome Biol. *19*,
922 64. 10.1186/s13059-018-1448-7.

923 64. Koestler, D.C., Jones, M.J., Usset, J., Christensen, B.C., Butler, R.A., Kobor, M.S., Wiencke,
924 J.K., and Kelsey, K.T. (2016). Improving cell mixture deconvolution by identifying optimal DNA
925 methylation libraries (IDOL). BMC Bioinformatics *17*, 120. 10.1186/s12859-016-0943-7.

926 65. Imai, C., Takimoto, H., Kurotani, K., Fudono, A., Tarui, I., Aoyama, T., Yago, S., Okamitsu, M.,
927 Miyasaka, N., and Sato, N. (2023). Diet Quality and Its Relationship with Weight Characteristics
928 in Pregnant Japanese Women: A Single-Center Birth Cohort Study. Nutrients *15*.
929 10.3390/nu15081827.

930 66. Imai, C., Takimoto, H., Fudono, A., Tarui, I., Aoyama, T., Yago, S., Okamitsu, M., Sasaki, S.,
931 Mizutani, S., Miyasaka, N., et al. (2021). Application of the Nutrient-Rich Food Index 9.3 and the
932 Dietary Inflammatory Index for Assessing Maternal Dietary Quality in Japan: A Single-Center
933 Birth Cohort Study. Nutrients *13*. 10.3390/nu13082854.

934 67. Cortes, M., Chen, M.J., Stachura, D.L., Liu, S.Y., Kwan, W., Wright, F., Vo, L.T., Theodore, L.N.,
935 Esain, V., Frost, I.M., et al. (2016). Developmental vitamin D availability impacts hematopoietic
936 stem cell production. Cell Rep. *17*, 458–468. 10.1016/j.celrep.2016.09.012.

937 68. Fraser, D., Kooh, S.W., Kind, H.P., Holick, M.F., Tanaka, Y., and DeLuca, H.F. (1973).
938 Pathogenesis of hereditary vitamin-D-dependent rickets. An inborn error of vitamin D metabolism
939 involving defective conversion of 25-hydroxyvitamin D to 1 alpha,25-dihydroxyvitamin D. N. Engl.
940 J. Med. *289*, 817–822. 10.1056/NEJM197310182891601.

941 69. Wientroub, S., Hagan, M.P., and Reddi, A.H. (1982). Reduction of hematopoietic stem cells and
942 adaptive increase in cell cycle rate in rickets. Am. J. Physiol. *243*, C303-6.
943 10.1152/ajpcell.1982.243.5.C303.

944 70. Gao, X., Xu, C., Asada, N., and Frenette, P.S. (2018). The hematopoietic stem cell niche: from
945 embryo to adult. Development *145*. 10.1242/dev.139691.

946 71. Taoudi, S., Bee, T., Hilton, A., Knezevic, K., Scott, J., Willson, T.A., Collin, C., Thomas, T.,
947 Voss, A.K., Kile, B.T., et al. (2011). ERG dependence distinguishes developmental control of
948 hematopoietic stem cell maintenance from hematopoietic specification. Genes Dev. *25*, 251–
949 262. 10.1101/gad.2009211.

950 72. Orkin, S.H., and Zon, L.I. (2008). Hematopoiesis: an evolving paradigm for stem cell biology.
951 Cell *132*, 631–644. 10.1016/j.cell.2008.01.025.

952 73. Baron, M.H., Isern, J., and Fraser, S.T. (2012). The embryonic origins of erythropoiesis in
953 mammals. Blood *119*, 4828–4837. 10.1182/blood-2012-01-153486.

954 74. Soares-da-Silva, F., Peixoto, M., Cumano, A., and Pinto-do-Ó, P. (2020). Crosstalk between the
955 hepatic and hematopoietic systems during embryonic development. Front. Cell Dev. Biol. *8*, 612.
956 10.3389/fcell.2020.00612.

957 75. Tavian, M., and Péault, B. (2005). Embryonic development of the human hematopoietic system.
958 Int. J. Dev. Biol. *49*, 243–250. 10.1387/ijdb.041957mt.

76. Elgormus, Y., Okuyan, O., and Uzun, H. (2023). The relationship between hematological indices as indicators of inflammation and 25-hydroxyvitamin D3 status in newborns. BMC Pediatr. *23*, 83. 10.1186/s12887-023-03903-8.

77. Xin, Y., Shao, Y., Mu, W., Li, H., Zhou, Y., and Wang, C. (2022). Accuracy of the neutrophil-to-lymphocyte ratio for the diagnosis of neonatal sepsis: a systematic review and meta-analysis. BMJ Open *12*, e060391. 10.1136/bmjopen-2021-060391.

78. Sumitro, K.R., Utomo, M.T., and Widodo, A.D.W. (2021). Neutrophil-to-Lymphocyte Ratio as an Alternative Marker of Neonatal Sepsis in Developing Countries. Oman Med. J. *36*, e214. 10.5001/omj.2021.05.

79. Panda, S.K., Nayak, M.K., Rath, S., and Das, P. (2021). The Utility of the Neutrophil-Lymphocyte Ratio as an Early Diagnostic Marker in Neonatal Sepsis. Cureus *13*, e12891. 10.7759/cureus.12891.

80. Workneh Bitew, Z., Worku, T., and Alemu, A. (2021). Effects of vitamin D on neonatal sepsis: A systematic review and meta-analysis. Food Sci. Nutr. *9*, 375–388. 10.1002/fsn3.2003.

81. Can, E., and Can, C. (2019). The value of neutrophil-to-lymphocyte ratio (NLR) and platelet-to-lymphocyte ratio (PLR) parameters in analysis with fetal malnutrition neonates. J. Perinat. Med. *47*, 775–779. 10.1515/jpm-2019-0016.

82. Chen, F., Marquez, H., Kim, Y.-K., Qian, J., Shao, F., Fine, A., Cruikshank, W.W., Quadro, L., and Cardoso, W.V. (2014). Prenatal retinoid deficiency leads to airway hyperresponsiveness in adult mice. J. Clin. Invest. *124*, 801–811. 10.1172/JCI70291.

83. O'Callaghan-Gordo, C., Kogevinas, M., Fthenou, E., Pedersen, M., Espinosa, A., Chalkiadaki, G., Daraki, V., Dermitzaki, E., Decordier, I., Georgiou, V., et al. (2017). Vitamin D insufficient levels during pregnancy and micronuclei frequency in peripheral blood T lymphocytes mothers and newborns (Rhea cohort, Crete). Clin. Nutr. *36*, 1029–1035. 10.1016/j.clnu.2016.06.016.

84. Andrews/Babraham Institute, S. (2010). FastQC: A quality control tool for high throughput sequence data. https://www.bioinformatics.babraham.ac.uk/projects/fastqc/.

85. Martin, M. (2011). Cutadapt removes adapter sequences from high-throughput sequencing reads. EMBnet j. *17*, 10. 10.14806/ej.17.1.200.

86. Dobin, A., Davis, C.A., Schlesinger, F., Drenkow, J., Zaleski, C., Jha, S., Batut, P., Chaisson, M., and Gingeras, T.R. (2013). STAR: ultrafast universal RNA-seq aligner. Bioinformatics *29*, 15–21. 10.1093/bioinformatics/bts635.

87. Wang, L., Wang, S., and Li, W. (2012). RSeQC: quality control of RNA-seq experiments. Bioinformatics *28*, 2184–2185. 10.1093/bioinformatics/bts356.

88. Yu, G., Wang, L.-G., Han, Y., and He, Q.-Y. (2012). clusterProfiler: an R package for comparing biological themes among gene clusters. OMICS *16*, 284–287. 10.1089/omi.2011.0118.

89. Stoeckius, M., Zheng, S., Houck-Loomis, B., Hao, S., Yeung, B.Z., Mauck, W.M., Smibert, P., and Satija, R. (2018). Cell Hashing with barcoded antibodies enables multiplexing and doublet detection for single cell genomics. Genome Biol. *19*, 224. 10.1186/s13059-018-1603-1.

997 90. Gao, S., Shi, Q., Zhang, Y., Liang, G., Kang, Z., Huang, B., Ma, D., Wang, L., Jiao, J., Fang, X.,
998 et al. (2022). Identification of HSC/MPP expansion units in fetal liver by single-cell
999 spatiotemporal transcriptomics. Cell Res. *32*, 38–53. 10.1038/s41422-021-00540-7.

1000 91. Lachmann, A., Xu, H., Krishnan, J., Berger, S.I., Mazloom, A.R., and Ma'ayan, A. (2010). ChEA:
1001 transcription factor regulation inferred from integrating genome-wide ChIP-X experiments.
1002 Bioinformatics *26*, 2438–2444. 10.1093/bioinformatics/btq466.

1003 92. Chen, E.Y., Tan, C.M., Kou, Y., Duan, Q., Wang, Z., Meirelles, G.V., Clark, N.R., and Ma'ayan,
1004 A. (2013). Enrichr: interactive and collaborative HTML5 gene list enrichment analysis tool. BMC
1005 Bioinformatics *14*, 128. 10.1186/1471-2105-14-128.

1006 93. Nishikawa, M., Yasuda, K., Takamatsu, M., Abe, K., Nakagawa, K., Tsugawa, N., Hirota, Y.,
1007 Tanaka, K., Yamashita, S., Ikushiro, S., et al. (2019). Generation of 1,25-dihydroxyvitamin D3 in
1008 Cyp27b1 knockout mice by treatment with 25-hydroxyvitamin D3 rescued their rachitic
1009 phenotypes. J. Steroid Biochem. Mol. Biol. *185*, 71–79. 10.1016/j.jsbmb.2018.07.012.

1010 94. Higashi, T., Awada, D., and Shimada, K. (2001). Simultaneous determination of 25-
1011 hydroxyvitamin D2 and 25-hydroxyvitamin D3 in human plasma by liquid chromatography-
1012 tandem mass spectrometry employing derivatization with a Cookson-type reagent. Biol. Pharm.
1013 Bull. *24*, 738–743. 10.1248/bpb.24.738.

1014 95. Houseman, E.A., Accomando, W.P., Koestler, D.C., Christensen, B.C., Marsit, C.J., Nelson,
1015 H.H., Wiencke, J.K., and Kelsey, K.T. (2012). DNA methylation arrays as surrogate measures of
1016 cell mixture distribution. BMC Bioinformatics *13*, 86. 10.1186/1471-2105-13-86.

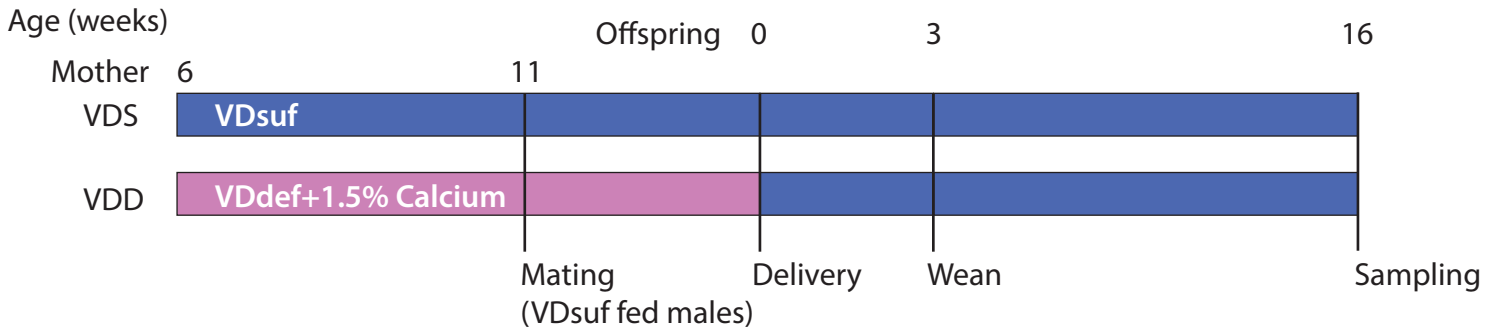
Age (weeks)
Offspring
0
3
16
Mother
6
11
VDS
VDsuf
VDD
VDdef+1.5% Calcium
Mating
(VDsuf fed males)
Delivery
Wean
Sampling

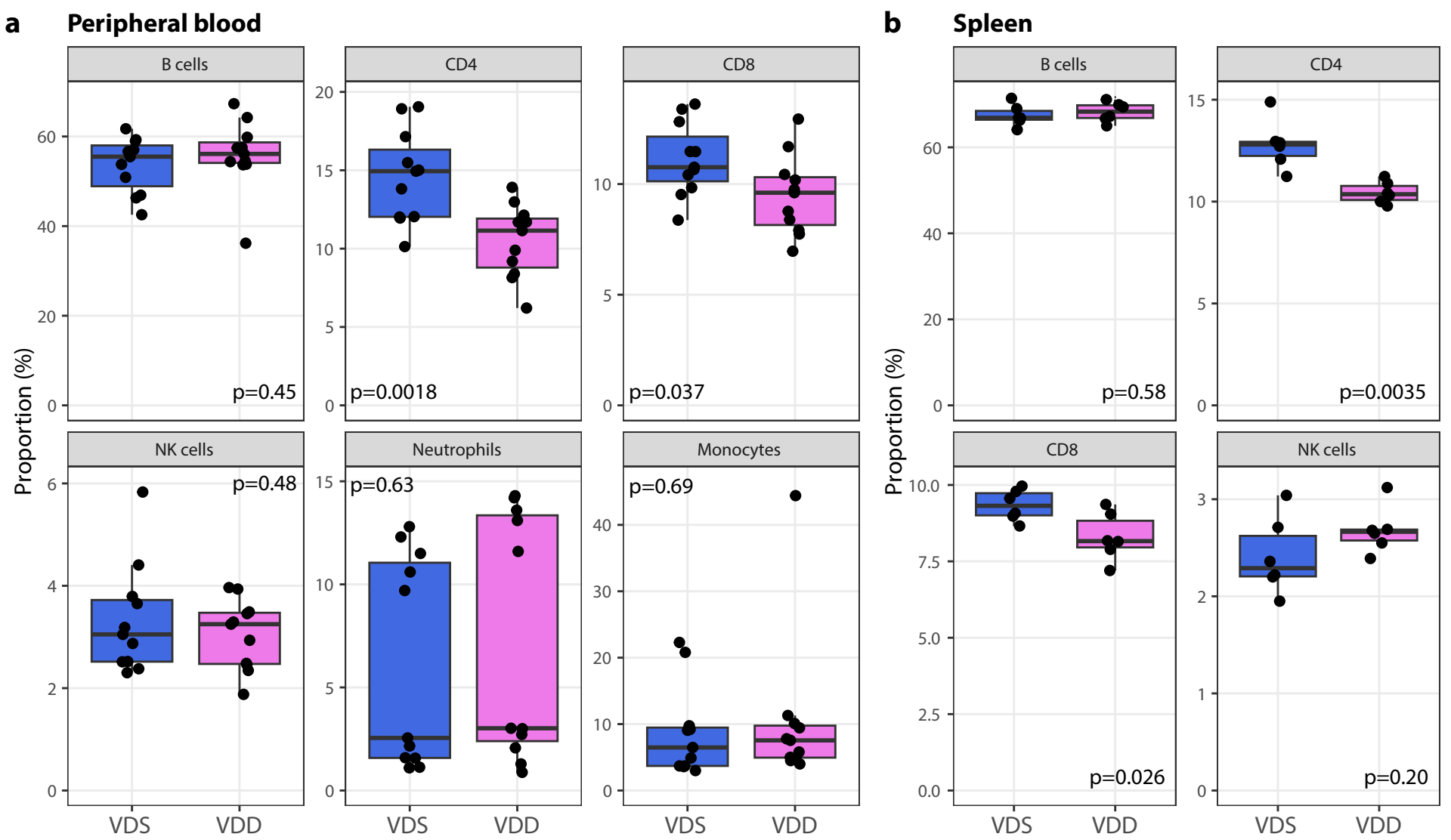
a
Peripheral blood
b
Spleen
B cells
CD4
CD8
NK cells
Neutrophils
Monocytes
Proportion (%)
p=0.45
p=0.0018
p=0.037
p=0.48
p=0.63
p=0.69
p=0.58
p=0.0035
p=0.026
p=0.20
VDS
VDD

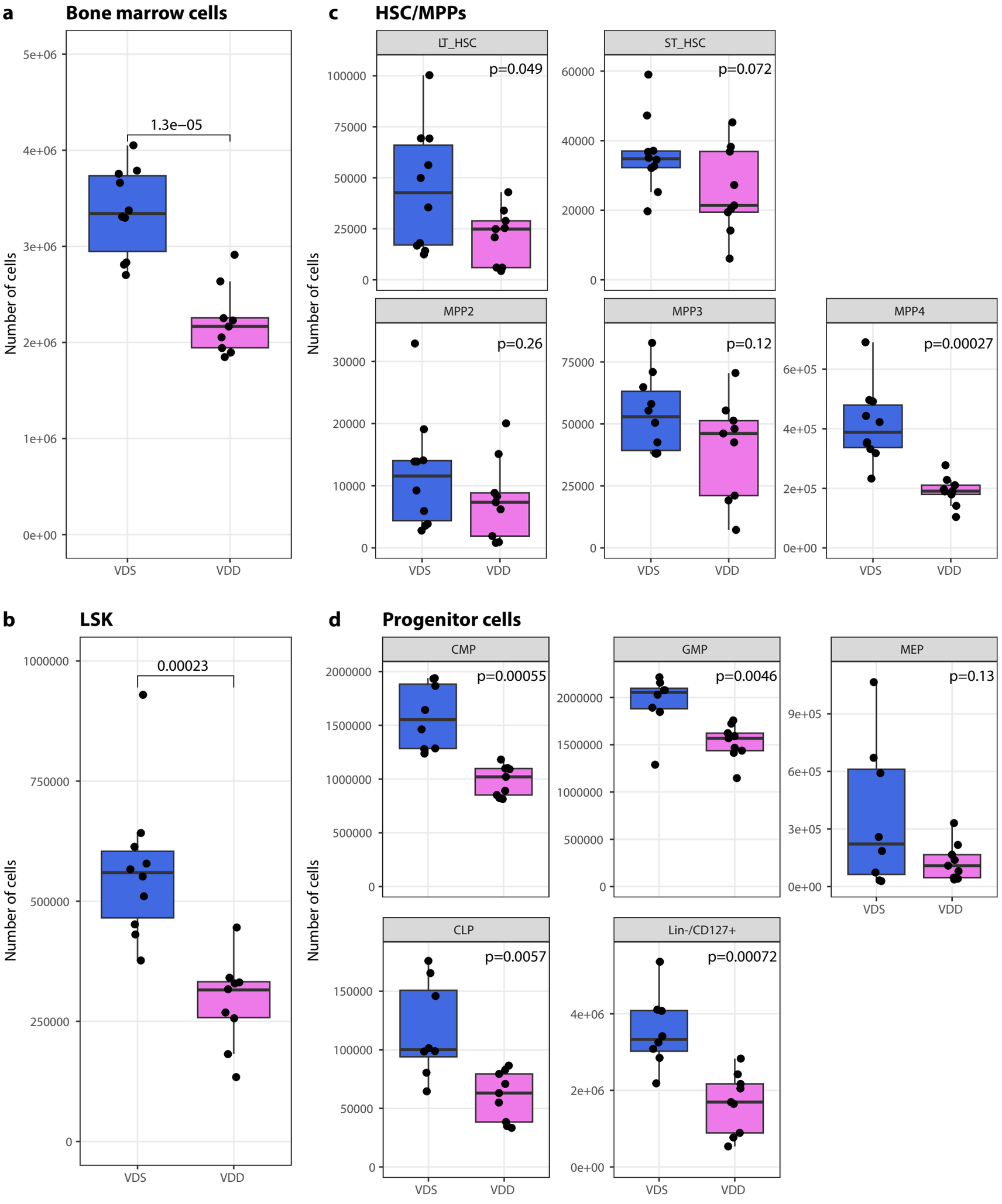
a
Bone marrow cells
1.3e−05
Number of cells
VDS
VDD
b
LSK
0.00023
c
HSC/MPPs
LT_HSC
p=0.049
ST_HSC
p=0.072
MPP2
p=0.26
MPP3
p=0.12
MPP4
p=0.00027
d
Progenitor cells
CMP
p=0.00055
GMP
p=0.0046
MEP
p=0.13
CLP
p=0.0057
Lin-/CD127+
p=0.00072

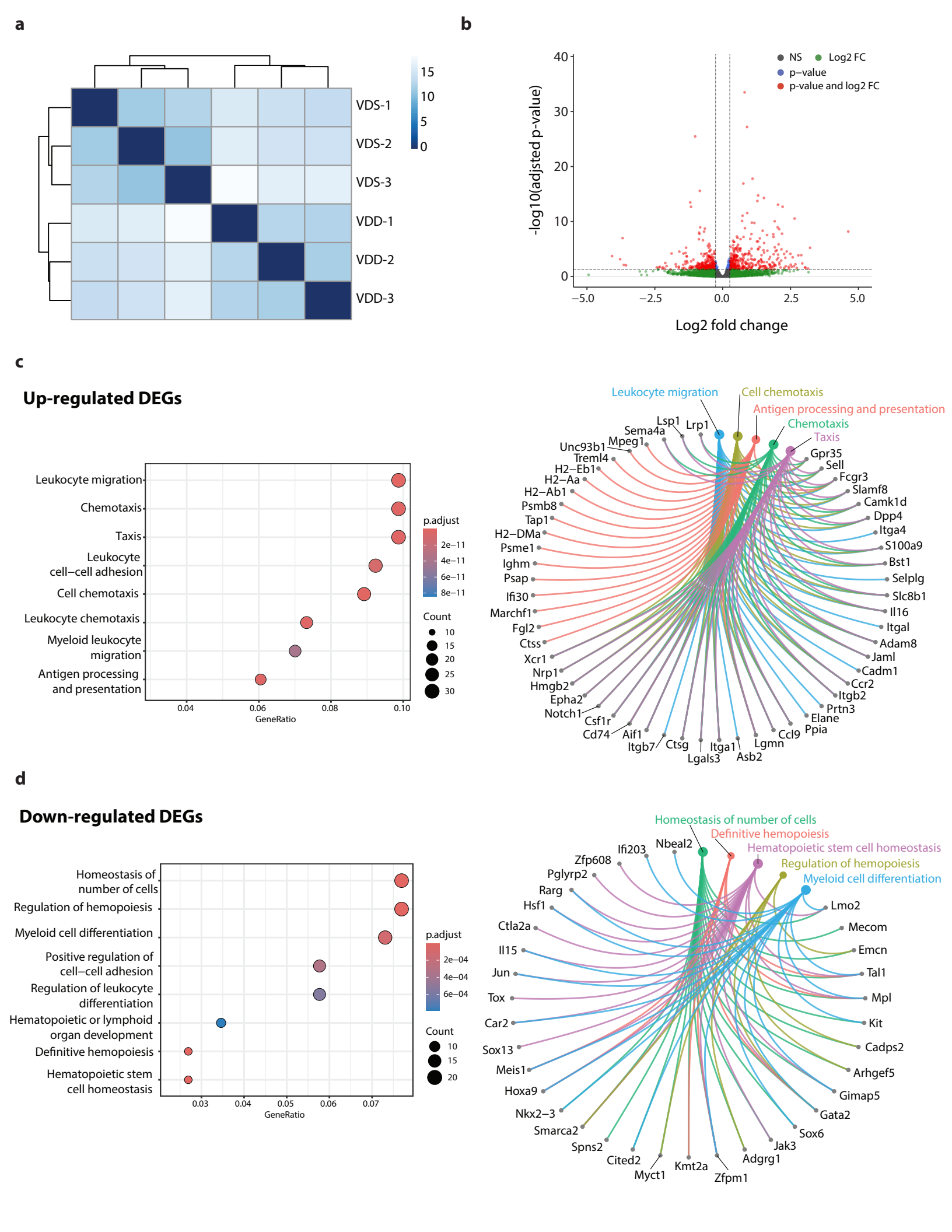
a
VDS-1
VDS-2
VDS-3
VDD-1
VDD-2
VDD-3
15
10
5
0
b
NS
Log2 FC
p-value
p-value and log2 FC
-log10(adjsted p-value)
Log2 fold change
c
Up-regulated DEGs
Leukocyte migration
Chemotaxis
Taxis
Leukocyte cell–cell adhesion
Cell chemotaxis
Leukocyte chemotaxis
Myeloid leukocyte migration
Antigen processing and presentation
GeneRatio
p.adjust
Count
Antigen processing and presentation
Chemotaxis
Taxis
d
Down-regulated DEGs
Homeostasis of number of cells
Regulation of hemopoiesis
Myeloid cell differentiation
Positive regulation of cell–cell adhesion
Regulation of leukocyte differentiation
Hematopoietic or lymphoid organ development
Definitive hemopoiesis
Hematopoietic stem cell homeostasis
GeneRatio
p.adjust
Count
Definitive hemopoiesis
Hematopoietic stem cell homeostasis
Regulation of hemopoiesis
Myeloid cell differentiation

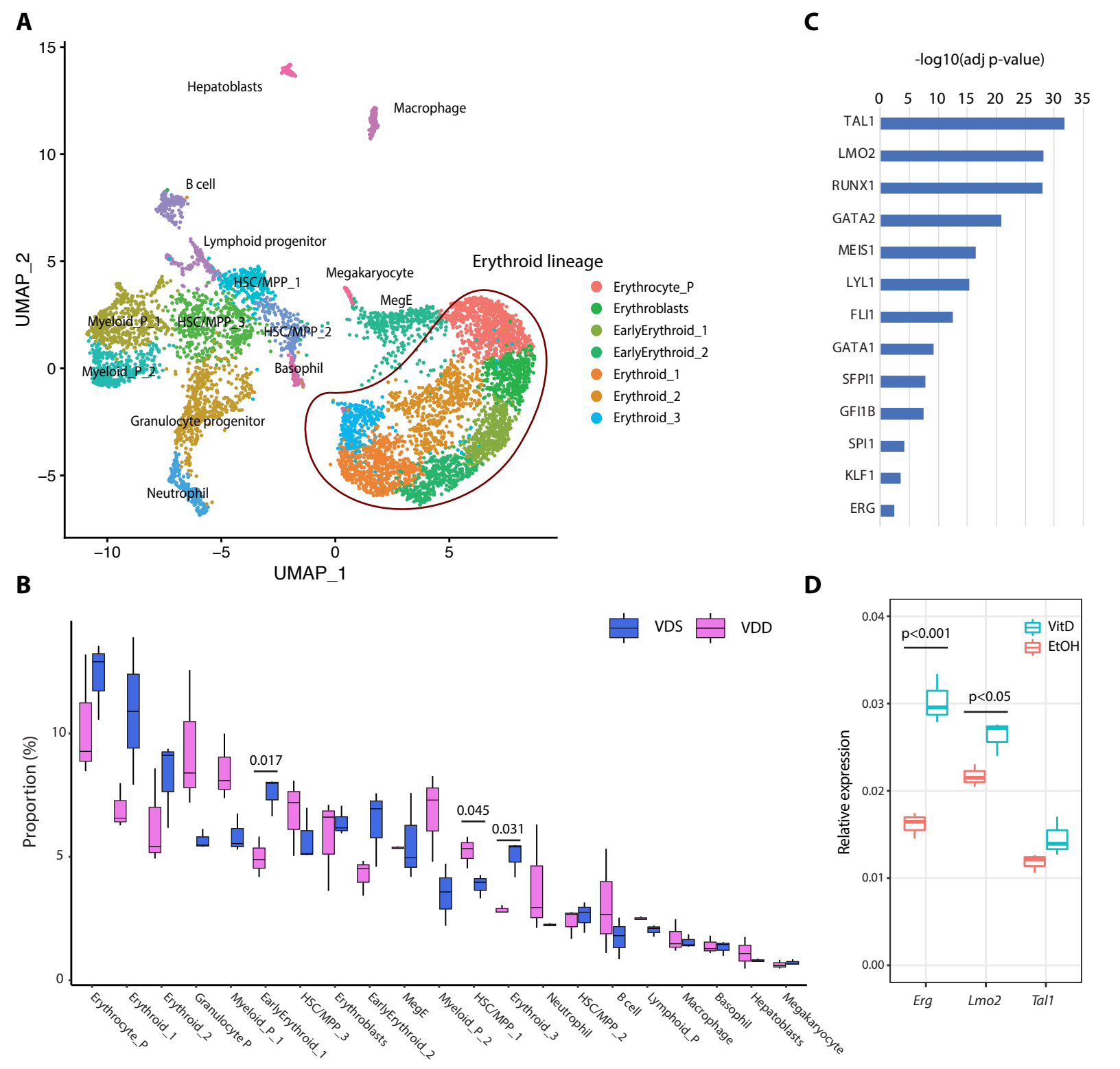
A
Hepatoblasts
Macrophage
B cell
Lymphoid progenitor
HSC/MPP_1
Megakaryocyte
MegE
Erythroid lineage
Myeloid_P_1
HSC/MPP_3
HSC/MPP_2
Myeloid_P_2
Basophil
Granulocyte progenitor
Neutrophil
UMAP_2
UMAP_1
Erythrocyte_P
Erythroblasts
EarlyErythroid_1
EarlyErythroid_2
Erythroid_1
Erythroid_2
Erythroid_3
C
-log10(adj p-value)
TAL1
LMO2
RUNX1
GATA2
MEIS1
LYL1
FLI1
GATA1
SFPI1
GFI1B
SPI1
KLF1
ERG
B
VDS
VDD
Proportion (%)
0.017
0.045
0.031
Erythrocyte_P
Erythroid_1
Erythroid_2
Granulocyte P
Myeloid_P_1
EarlyErythroid_1
HSC/MPP_3
Erythroblasts
EarlyErythroid_2
MegE
Myeloid_P_2
HSC/MPP_1
Erythroid_3
Neutrophil
HSC/MPP_2
B cell
Lymphoid_P
Macrophage
Basophil
Hepatoblasts
Megakaryocyte
D
VitD
EtOH
p<0.001
p<0.05
Relative expression
Erg
Lmo2
Tal1

**a**

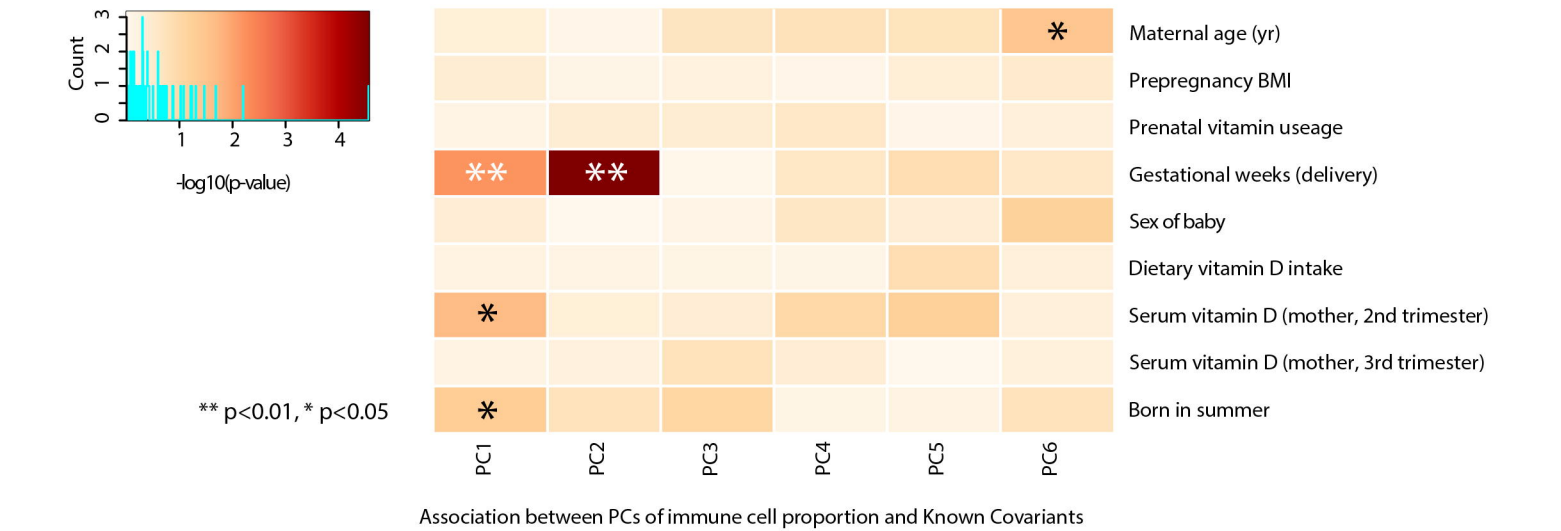
Count
0
1
2
3
1
2
3
4
-log10(p-value)
Maternal age (yr)
Prepregnancy BMI
Prenatal vitamin useage
Gestational weeks (delivery)
Sex of baby
Dietary vitamin D intake
Serum vitamin D (mother, 2nd trimester)
Serum vitamin D (mother, 3rd trimester)
Born in summer
** p<0.01, * p<0.05
PC1
PC2
PC3
PC4
PC5
PC6
Association between PCs of immune cell proportion and Known Covariants

**b**

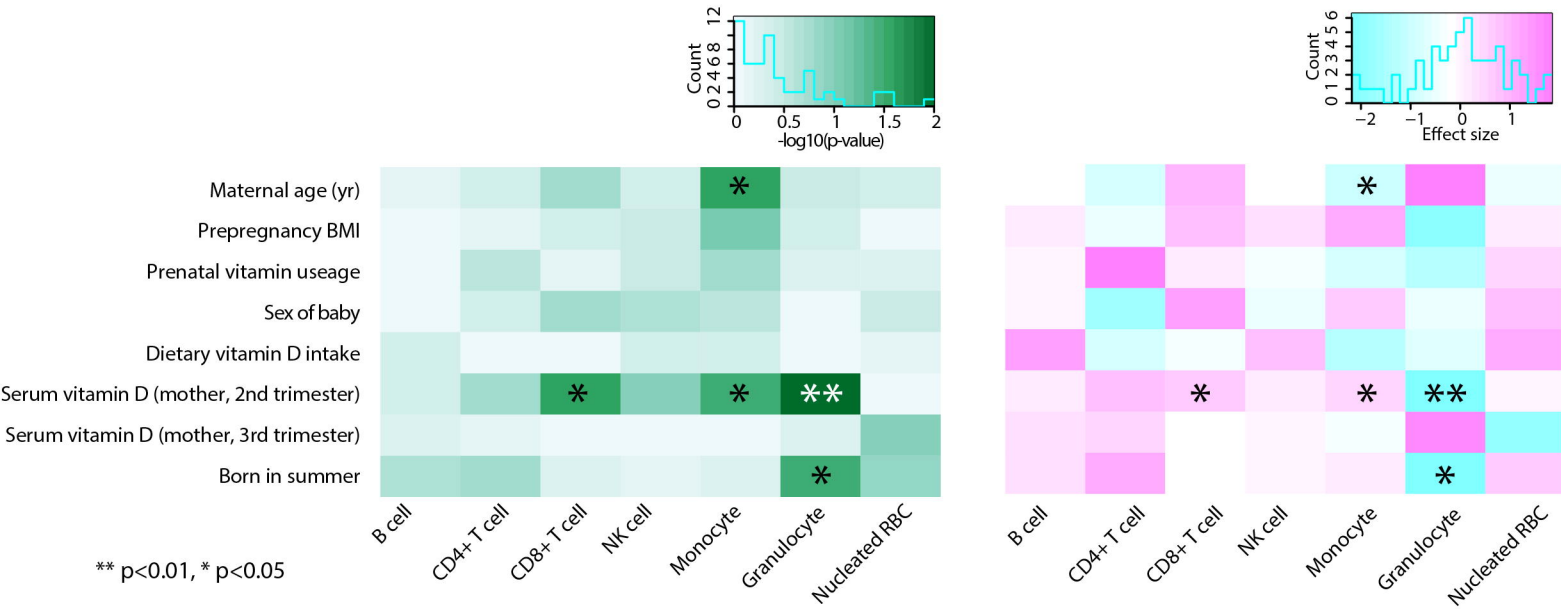
Count
0
2
4
6
8
12
0
0.5
1
1.5
2
-log10(p-value)
Count
0
1
2
3
4
5
6
−2
−1
0
1
Effect size
Maternal age (yr)
Prepregnancy BMI
Prenatal vitamin useage
Sex of baby
Dietary vitamin D intake
Serum vitamin D (mother, 2nd trimester)
Serum vitamin D (mother, 3rd trimester)
Born in summer
B cell
CD4+ T cell
CD8+ T cell
NK cell
Monocyte
Granulocyte
Nucleated RBC
** p<0.01, * p<0.05